ENGINEERING OF
BIOMATERIALS
INŻYNIERIA BIOMATERIAŁÓW
JOURNAL OF POLISH SOCIETY FOR BIOMATERIALS AND FACULTY OF MATERIALS SCIENCE AND CERAMICS AGH-UST
CZASOPISMO POLSKIEGO STOWARZYSZENIA BIOMATERIAŁÓW I WYDZIAŁU INŻYNIERII MATERIAŁOWEJ I CERAMIKI AGH

Number 135
Numer 135
Volume XIX
Rok XIX

APRIL 2016
KWIECIEŃ 2016

ISSN 1429-7248

PUBLISHER:
WYDAWCA:

Polish Society for Biomaterials in Krakow
Polskie Stowarzyszenie Biomateriałów w Krakowie

EDITORIAL COMMITTEE:
KOMITET REDAKCYJNY:

Editor-in-Chief
Redaktor naczelny
Jan Chłopek

Editor
Redaktor
Elżbieta Pamuła

Secretary of editorial
Sekretarz redakcji
Design
Projekt
Katarzyna Trała
Augustyn Powroźnik

ADDRESS OF EDITORIAL OFFICE:
ADRES REDAKCJI:

AGH-UST
30/A3, Mickiewicz Av.
30-059 Krakow, Poland
Akademia Górniczo-Hutnicza
al. Mickiewicza 30/A-3
30-059 Kraków

Issue: 250 copies
Nakład: 250 egz.

Scientific Publishing House AKAPIT
Wydawnictwo Naukowe AKAPIT
e-mail: wn@akapit.krakow.pl

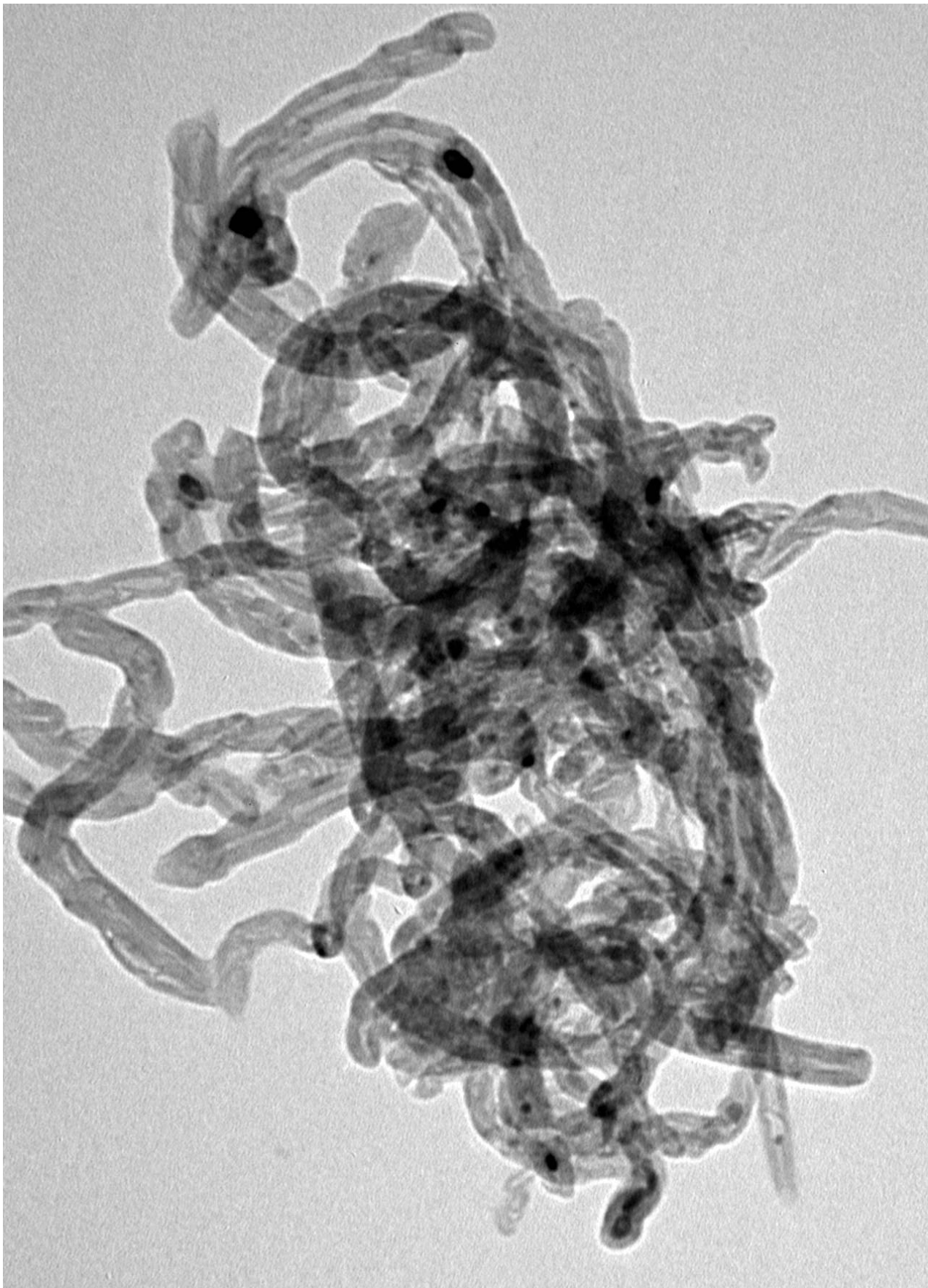

ENGINEERING OF BIOMATERIALS

EDITORIAL BOARD
KOMITET REDAKCYJNY

INTERNATIONAL EDITORIAL BOARD
MIĘDZYNARODOWY KOMITET REDAKCYJNY

ENGINEERING OF BIOMATERIALS

Wskazówki dla autorów

1. Prace do opublikowania w kwartalniku „Engineering of Biomaterials / Inżynieria Biomateriałów" przyjmowane będą wyłącznie z tłumaczeniem na język angielski. Obcokrajowców obowiązuje tylko język angielski.
2. Wszystkie nadsyłane artykuły są recenzowane.
3. Materiały do druku prosimy przysyłać na adres e-mail: kabe@agh.edu.pl.
4. Struktura artykułu:
   • TYTUŁ • Autorzy i instytucje • Streszczenie (200-250 słów) • Słowa kluczowe • Wprowadzenie • Materiały i metody • Wyniki i dyskusja • Wnioski • Podziękowania • Piśmiennictwo
5. Autorzy przesyłają pełną wersję artykułu, łącznie z ilustracjami, tabelami, podpisami i literaturą w jednym pliku. Ilustracje, tabele, podpisy i literatura powinny być umieszczone również w wersji angielskiej. Artykuł w tej formie przesyłany jest do recenzentów. Dodatkowo autorzy proszeni są o przesłanie materiałów ilustracyjnych (rysunki, schematy, fotografie, wykresy) w oddzielnych plikach (format np. .jpg, .gif., .tiff, .bmp). Rozdzielczość rysunków min. 300 dpi. Wszystkie rysunki i wykresy powinny być czarno-białe lub w odcieniach szarości i ponumerowane cyframi arabskimi. W tekście należy umieścić odnośniki do rysunków i tabel. W tabelach i na wykresach należy umieścić opisy polskie i angielskie.
6. Na końcu artykułu należy podać wykaz piśmiennictwa w kolejności cytowania w tekście i kolejno ponumerowany.
7. Redakcja zastrzega sobie prawo wprowadzenia do opracowań autorskich zmian terminologicznych, poprawek redakcyjnych, stylistycznych, w celu dostosowania artykułu do norm przyjętych w naszym czasopiśmie. Zmiany i uzupełnienia merytoryczne będą dokonywane w uzgodnieniu z autorem.
8. Opinia lub uwagi recenzentów będą przekazywane Autorowi do ustosunkowania się. Nie dostarczenie poprawionego artykułu w terminie oznacza rezygnację Autora z publikacji pracy w naszym czasopiśmie.
9. Za publikację artykułów redakcja nie płaci honorarium autorskiego.
10. Adres redakcji:
    Czasopismo
    „Engineering of Biomaterials / Inżynieria Biomateriałów"
    Akademia Górniczo-Hutnicza im. St. Staszica
    Wydział Inżynierii Materiałowej i Ceramiki
    al. Mickiewicza 30/A-3, 30-059 Kraków
    tel. (48) 12 617 25 03, 12 617 25 61
    tel./fax: (48) 12 617 45 41
    e-mail: chlopek@agh.edu.pl, kabe@agh.edu.pl

Szczegółowe informacje dotyczące przygotowania manuskryptu oraz procedury recenzowania dostępne są na stronie internetowej czasopisma:
www.biomat.krakow.pl

Warunki prenumeraty

Zamówienie na prenumeratę prosimy przesyłać na adres:
apowroz@agh.edu.pl, tel/fax: (48) 12 617 45 41
Cena pojedynczego numeru wynosi 20 PLN
Konto:
Polskie Stowarzyszenie Biomateriałów
30-059 Kraków, al. Mickiewicza 30/A-3
ING Bank Śląski S.A. O/Kraków
nr rachunku 63 1050 1445 1000 0012 0085 6001

Instructions for authors

1. Papers for publication in quarterly journal „Engineering of Biomaterials / Inżynieria Biomateriałów" should be written in English.
2. All articles are reviewed.
3. Manuscripts should be submitted to editorial office by e-mail to kabe@agh.edu.pl.
4. A manuscript should be organized in the following order:
• TITLE • Authors and affiliations • Abstract (200-250 words) • Keywords (4-6) • Introduction • Materials and Methods • Results and Discussions • Conclusions • Acknowledgements • References
5. All illustrations, figures, tables, graphs etc. preferably in black and white or grey scale should be additionally sent as separate electronic files (format .jpg, .gif., .tiff, .bmp). High-resolution figures are required for publication, at least 300 dpi. All figures must be numbered in the order in which they appear in the paper and captioned below. They should be referenced in the text. The captions of all figures should be submitted on a separate sheet.
6. References should be listed at the end of the article. Number the references consecutively in the order in which they are first mentioned in the text.
7. The Editors reserve the right to improve manuscripts on grammar and style and to modify the manuscripts to fit in with the style of the journal. If extensive alterations are required, the manuscript will be returned to the authors for revision.
8. Opinion or notes of reviewers will be transferred to the author. If the corrected article will not be supplied on time, it means that the author has resigned from publication of work in our journal.
9. Editorial does not pay author honorarium for publication of article.
10. Address of editorial office:
    Journal
    „Engineering of Biomaterials / Inżynieria Biomateriałów"
    AGH University of Science and Technology
    Faculty of Materials Science and Ceramics
    30/A-3, Mickiewicz Av., 30-059 Krakow, Poland
    tel. (48) 12) 617 25 03, 12 617 25 61
    tel./fax: (48) 12 617 45 41
    e-mail: chlopek@agh.edu.pl, kabe@agh.edu.pl

Detailed information concerning manuscript preparation and review process are available at the journal's website:
www.biomat.krakow.pl

Subscription terms

Subscription rates:
Cost of one number: 20 PLN
Payment should be made to:
Polish Society for Biomaterials
30/A3, Mickiewicz Av.
30-059 Krakow, Poland
ING Bank Slaski S.A.
account no. 63 1050 1445 1000 0012 0085 6001

25th Biomaterials in Medicine and Veterinary Medicine

13 – 16 October 2016 Rytro, Poland

Anniversary Conference

WE HAVE A LOT TO CELEBRATE!

25th

ANNIVERSARY CONFERENCE

20

YEARS OF THE POLISH SOCIETY FOR BIOMATERIALS

SUBMIT YOUR ABSTRACT AND FULL PAPER

WWW.BIOMAT.AGH.EDU.PL

SPIS TREŚCI

CONTENTS

Wersja papierowa czasopisma „Engineering of Biomaterials / Inżynieria Biomateriałów" jest jego wersją pierwotną
Printed version of „Engineering of Biomaterials / Inżynieria Biomateriałów" is a primary version of the journal

Wydanie dofinansowane przez Ministra Nauki i Szkolnictwa Wyższego
Edition financed by the Minister of Science and Higher Education

ENGINEERING OF BIOMATERIALS

ADHESION, GROWTH AND OSTEOGENIC DIFFERENTIATION OF HUMAN BONE MARROW MESENCHYMAL STEM CELLS ON POSITIVELY AND NEGATIVELY CHARGED AND UNCHARGED FERROELECTRIC CRYSTAL SURFACES

Marta Vandrovcova[1], Lucie Bacakova[1]*, Premysl Vanek[2], Jan Petzelt[2]

[1] Institute of Physiology of the Czech Academy of Sciences, Videnska 1083, CZ-14220 Prague, Czech Republic
[2] Institute of Physics of the Czech Academy of Sciences, Na Slovance 2, CZ-18221 Prague, Czech Republic
*e-mail: Lucie.Bacakova@fgu.cas.cz

Abstract

The cell-material interaction is significantly influenced by the physicochemical properties of the material surface, including its electrical charge. In this study, the effect of the surface polarity of ferroelectric $LiNbO_3$ single crystals on the adhesion, growth and osteogenic differentiation of human bone marrow mesenchymal stem cells was investigated. The cells were cultured on the normal-to-plane poled and in-plane poled plates resulting in positive, negative and zero surface charge. The number of initially adhering cells on day 1 after seeding, their spreading, shape, and their metabolic activity, production of type I collagen, activity of alkaline phosphatase and mineralization in the following days of cultivation (days 6 and 20) were comparable on all three tested surfaces. However, significant differences were found in the expression of mRNA for type I collagen, alkaline phosphatase and osteocalcin, i.e. an early, medium-term and late markers of osteogenic cell differentiation, respectively. On day 20, the expression of type I collagen was significantly lower in cells on negatively-charged than on non-charged surfaces. Moreover, the expression of alkaline phosphatase and osteocalcin was higher in cells on positively-charged than on negatively-charged surfaces. These differences were generally more pronounced in standard cell culture medium than in osteogenic medium, which could, at least partly, mask the influence of the material surface properties on the cell behaviour. Thus, positively-charged $LiNbO_3$ surfaces seemed to be more suitable for the osteogenic differentiation of bone marrow mesenchymal stem cells than the negatively-charged surfaces.

Keywords: *electroactive ceramics, surface charge, cell number, resazurin, type I collagen, alkaline phosphatase, osteocalcin, bone matrix mineralization*

[Engineering of Biomaterials 135 (2016) 2-7]

Introduction

Cell-biomaterial interaction strongly depends on the physical and chemical properties of the material surface, such as its polarity, wettability, roughness and topography, rigidity and deformability, pH, electrical charge and conductivity (for a review, see [1]). In order to modulate the physicochemical properties of the material surface, a wide range of the material surface modifications have been developed, including irradiation with ions or ultraviolet light, plasma treatment, etching in acids or alkalis, grinding, polishing, electric discharge machining, shot peening, and particularly coating with various films based on oxides, nitrides, carbon materials or ceramics (for a review, see [1,2]).

In this study, we concentrated on the adhesion, growth and osteogenic differentiation of human bone marrow mesenchymal stem cells on electrically-charged surfaces with different polarization – positive or negative. There is a controversy among the studies dealing with the influence of the positive or negative charge on the cell behaviour. One group of studies reported that the positive charge was more advantageous for the cell adhesion, growth and differentiation. For example, the attachment and spreading of osteoblasts and fibroblasts on positively charged 2-hydroxytheythylmethacrylate and poly(ethylene glycol) hydrogels were higher than on the negatively charged and electroneutral surfaces [3]. Similarly, the positive charge on hydroxyapatite/TiO_2 hybrid surfaces increased the number of rat bone marrow-derived osteoblast-like cells cultured on these surfaces [4].

However, another group of studies came to the opposite conclusion – negative charge is better for the colonization of materials with cells *in vitro* and the material osseointegration *in vivo*. For example, negatively charged hydroxyapatite and β-tricalcium phosphate surfaces enhanced the adhesion and proliferation of human fetal osteoblasts, extracellular matrix formation by these cells, and the matrix mineralization in comparison with the positively charged and non-charged surfaces [5]. The negative surface charge of electrically-polarized hydroxyapatite ceramics was associated with increased osteobonding activity of this material after its implantation into tibial and femoral diaphyses of rabbits *in vivo* [6].

Finally, some studies found that there was no significant difference between positively and negatively charged materials in supporting the growth and differentiation of osteogenic cells [7,8].

Our earlier studies performed on thermally oxidized Ti, Nb and TiNb surfaces suggested that the positive charge of the material surface promoted the cell growth, while the negative charge supported the osteogenic cell differentiation [9,10]. An explanation was that the positively charged surfaces improved the adsorption of the negatively charged proteins mediating the cell adhesion, while the negatively charged surfaces adsorbed more Ca^{2+} ions, and thus promote the bone matrix mineralization [4,5]; for a review, see [1,10].

In this study, we investigated the adhesion, growth and osteogenic cell differentiation in human bone marrow mesenchymal stem cells cultured on poled electroactive ferroelectric $LiNbO_3$ single crystalline plates with positive or negative surface charge due to polarization perpendicular to the surface or with zero surface charge when polarization is parallel to the surface. The cell behaviour was evaluated in terms of the cell number, metabolic activity, markers of osteogenic cell differentiation (type I collagen, alkaline phosphatase and osteocalcin) and the bone matrix mineralization.

Our earlier study, performed on human osteoblast-like Saos-2 cells cultured on positively and negatively charged $LiNbO_3$ surfaces, showed that the cell behavior tended to be slightly better on positively-charged surfaces [11]. Since the Saos-2 cells are a cell line of osteosarcoma origin, which may be less sensitive to the material surface properties than primocultured and low-passaged cells, this study intend to verify the results obtained on Saos-2 cells on commercially available primary human mesenchymal bone marrow stem cells (passage 2).

Materials and Methods

Samples for cell experiments

The study was carried out on commercially available $LiNbO_3$ substrates (MTI Corporation). The materials were supplied in the following form: single crystalline plates, optical grade, dimensions 10×10×0.5 mm^3, two-sides polished, surface roughness <0.8 nm (determined by AFM), (0001) orientation poled perpendicularly to the surface (one surface with the positive charge and the opposite one with the negative charge) and (0100) orientation poled parallel to the surface with zero charge due to the polarization. The polarity of the surface was determined using the d_{33} meter (piezoelectric coefficient d_{33} = ± 23 pC N^{-1}). The measurements of zeta-potential, performed in our earlier study, showed that at near-physiological pH (i.e. pH ~6), the zeta potential was less negative on positively-charged than on negatively-charged $LiNbO_3$ surfaces [11].

Cell seeding

The samples were sterilized by 70% ethanol for 2 hours, inserted into 24-well cell culture plates (TPP, Switzerland; inner well diameter 15 mm) and seeded with human bone marrow mesenchymal stem cells (ScienCell Research Laboratories, Cat. No. 7500, passage 2). Each well contained 19 000 cells (approximately 10 000 cells/cm^2) and 1 ml of Mesenchymal Stem Cell Medium (MSCM, ScienCell Research Laboratories, Cat. No. 7501). After 6 days, when the cells reached confluence, one half of samples received osteogenic differentiation medium which was composed of α-MEM (Gibco, Cat. No. 11900-016), dexamethasone (10nM; Sigma-Aldrich, Cat. No. D1530-10UG), β-glycerolphosphate (20mM; Sigma-Aldrich, Cat. No. G9422) and ascorbic acid (50 μM; Sigma-Aldrich, Cat. No. 49752-10G). The second half of samples received α-MEM (Gibco, Cat. No. 11900-016). All the media contained foetal bovine serum (15%; Sigma-Aldrich, Cat. No. F7524-500ML), L-Glutamine (2mM; Gibco, Cat. No. A2916801) and gentamicin (40 μg/ml; LEK).

Cell number

The cell number was evaluated on day 1 as an important indicator of the initial cell adhesion. The cells were rinsed in phosphate-buffered saline (PBS), fixed with frozen 70% ethanol (-20°C) for 10 min and stained for 1 h with a combination of two fluorescence dyes, namely Hoechst #33258 (5 μg/mL; Sigma-Aldrich, Cat. No. B1155-25MG), which stains the cell nuclei, and Texas Red C_2-maleimide (1 ng/mL; Life Technologies, Cat. No. T6008), which stains the cell membrane and cytoplasm. The cells were then counted on microphotographs, and their morphology, i.e. the shape and spreading, was also evaluated.

Metabolic activity of cells

On the days 6 and 20, the cell number was estimated using the conversion of resazurin (Sigma-Aldrich, Cat. No. R7017) into fluorescent resorufin by viable and metabolically active cells. Briefly, the stock solution of the resazurin (4 mM) was added to the medium without phenol red to the final concentration of 40 μM. 1 mL of solution was added to the cells washed with PBS in order to remove formal medium. After 4-hour incubation at 37°C, the fluorescence was measured (Ex/Em = 530/590 nm) and corrected to background control (solvent mixture without cells) on a Synergy™ HT Multi-Mode Microplate reader (BioTek, USA). The cell number was recalculated per the substrate area (1 cm^2).

Type I collagen production

The total amount of collagen (i.e., an important component of the bone matrix) produced by the cells, i.e., intracellular collagen and collagen deposited on the tested materials, was determined using a Sircol kit (Biocolor Ltd., Carrickfergus, UK) on day 20 after cell seeding (6 days in MSCM + 14 days in differentiation medium or 6 days in MSCM + 14 days in α-MEM). The collagen was recovered by acid–pepsin digestion. The cells were rinsed with PBS, harvested with a cell scraper in 700 μL of pepsin solution (1 mg/mL dissolved in 0.5 M acetic acid), and lysed overnight at 4°C. The lysates were centrifuged and the supernatants were concentrated according to the Sircol kit manufacturer's protocol. Finally, the Sircol dye was bound to the isolated collagen, was dissolved, and the absorbance of the colored solution was measured. The absorbance was measured using a VersaMax ELISA Microplate Reader (Molecular Devices LLC) in Nunc-Immuno MicroWell 96-well cell culture plates (Sigma-Aldrich) with wavelength at 555 nm. The amount of total collagen was adjusted to the cell metabolic activity per sample.

Alkaline phosphatase (ALP) activity

The influence of the electrical polarization of the materials on the activity of alkaline phosphatase (ALP), i.e. an enzyme participating in bone matrix mineralization, in hMSCs was studied. After 20 days of cultivation (6 days in MSCM + 14 days in differentiation medium or 6 days in MSCM + 14 days in α-MEM), the cell layers were twice washed with PBS, and then the substrate solution (0.1 mg/mL p-nitrophenyl phosphate in substrate buffer [50 mM glycine, 1 mM $MgCl_2$, pH 10.5]) (Sigma-Aldrich) was added directly to the cells. The reaction was performed for 10 min at room temperature; the substrate solution was then removed and mixed with the same volume of the 1 M NaOH solution. The absorbance (at 405 nm) of the samples was measured together with the absorbance of the known concentrations of p-nitrophenol diluted in 0.02 M NaOH (9-90 μM) (Sigma-Aldrich). The results were normalized to the cell metabolic activity per sample.

Calcium deposition

The influence of the material surface polarization on calcium deposition by hMSCs was studied. After 20 days of cultivation (6 days in MSCM + 14 days in osteogenic differentiation medium or 6 days in MSCM + 14 days in α-MEM) the cell layers were rinsed with PBS, dried, and lysed in 0.5 M HCl for 24 h at 4°C. The calcium in the cell lysates and standards was directly determined by using the Calcium Colorimetric Assay (Sigma-Aldrich, Cat. No. MAK022-1KT) according to the manufacturer's protocol. The results were normalized to the cell metabolic activity per sample.

TABLE 1. Oligonucleotide primers for RT-PCR amplifications.

Gene	Primer sequence	Product size (bp)
ALP	Forward: 5′-GACCCTTGACCCCCACAAT-3′	68
	Reverse: 5′-GCTCGTACTGCATGTCCCCT-3′	
Collagen type I	Forward: 5′-CAGCCGCTTCACCTACAGC-3′	83
	Reverse: 5′-TTTTGTATTCAATCACTGTCTTGCC-3′	
OC	Forward: 5’-GAAGCCCAGCGGTGCA-3’	70
	Reverse: 5’-CACTACCTCGCTGCCCTCC-3’	
GAPDH	Forward: 5′-TGCACCACCAACTGCTTAGC-3′	87
	Reverse: 5′-GGCATGGACTGTGGTCATGAG-3′	

Real-time Q-PCR of markers of osteogenic cell differentiation

Real-time quantitative PCR (Q-PCR) was used to determine the effect of charge on the level of expression of genes for type I collagen, ALP and OC. Cells were grown on the tested materials in the growth or differentiation media for 20 days. Total RNA was extracted from MSCs using Total RNA purification Micro Kit (NORGENE Biotek Corp, Cat. No. 35300). The mRNA concentration was measured using NanoPhotometer™ S/N (IMPLEN). The cDNA was synthesized with the ProtoScript®M-MuLV First Strand cDNA Synthesis kit (New England BioLabs, Cat. No. E6300S) using 250 ng of total RNA and oligo-dT primers. The reaction was performed in T-Personal Therocycler (Biometra). Q-PCR primers were purchased from Generi Biotech Ltd. and are listed in TABLE 1. The primers were designed according to the literature (TABLE 1). Real-time quantitative PCR was performed using SYBR Green (Roche) in the total reaction volume to 20 µL and iCycler detection system (iQ™ 5 Multicolor Real-Time PCR Detection System, Bio-Rad) with cycling parameters of 10 min at 95°C, then 40 cycles of 15 s at 95°C and 1 min at 60°C, followed by a melt curve. Assays were conducted in quadruplicates. Data were analysed by the $2^{-\Delta\Delta Ct}$ method. The point at which the PCR product was first detected above a fixed threshold (termed cycle threshold, C_t), was determined for each sample. Changes in the expression of target genes were calculated using the equation:

$$\Delta\Delta C_t = (C_t^{target} - C_t^{GAPDH})_{sample} - (C_t^{target} - C_t^{GAPDH})_{calibrator}$$

Glyceraldehyde 3-phosphate dehydrogenase (GAPDH) was used as a housekeeping gene and data was normalized to the expression levels of cells grown on polystyrene in α-MEM medium (PS norm, calibrator).

Statistical evaluation

Cell number data were presented as mean ± S.E.M. from 36 measurements. The quantitative data (metabolic activity, ALP activity, type I collagen production, Ca deposition) were presented as mean ± S.D. (Standard Deviation) from 2-3 measurements. PCR data was presented as mean ± S.D. from 4 measurements. The statistical analyses were performed using SigmaStat (Jandel Corporation, USA). Multiple comparison procedures were made by the One-Way Analysis of Variance (ANOVA), Student-Newman-Keuls method. The value $p \leq 0.05$ was considered significant.

Results and Discussions

The cell number on day 1 after seeding did not differ significantly among the tested groups, although in average, it was slightly higher on positively-charged $LiNbO_3$ surfaces than on the negatively-charged surfaces (FIG. 1 A). The cells on all tested surfaces were of similar morphology, i.e. mostly polygonal and well-spread (FIG. 2). On days 6 and 20 of cultivation, the cell metabolic activity, i.e. an indicator of cell number, was similar on all tested surfaces (FIG. 1 B, C). At the same time, the two different types of cultivation media (i.e., standard growth medium and differentiation medium) did not cause any significant difference in the metabolic activity of cells on day 20 (FIG. 1 C).

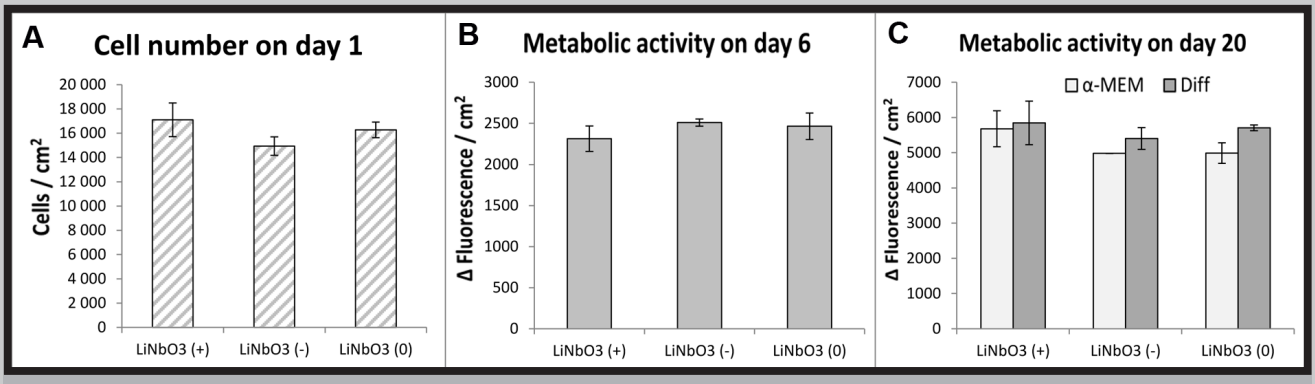

FIG. 1. Number (A) and metabolic activity (B, C) of human bone marrow mesenchymal stem cells on day 1, day 6, and day 20 after seeding on positively charged (+), negatively charged (-) and uncharged (0) $LiNbO_3$ surfaces. A: Mean ± S.E.M. from three samples (in total 36 values); B, C: Mean ± S.D. from three samples for each experimental group and time interval. C: For the last 14 days, the cells were cultured in standard medium (α-MEM) or osteogenic medium (Diff).

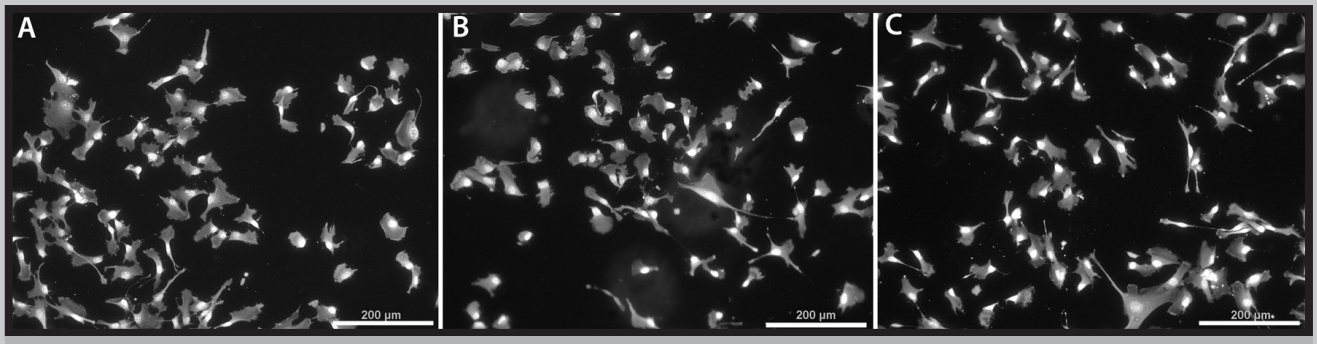

FIG. 2. Morphology of human bone marrow mesenchymal stem cells on day 1 after seeding on positively charged (A), negatively charged (B) and uncharged (C) $LiNbO_3$ samples. Cells stained with a combination of Hoechst #33258 and Texas Red C_2-maleimide. Olympus IX 51 microscope, objective 10x, DP 70 digital camera, scale bar = 200 µm.

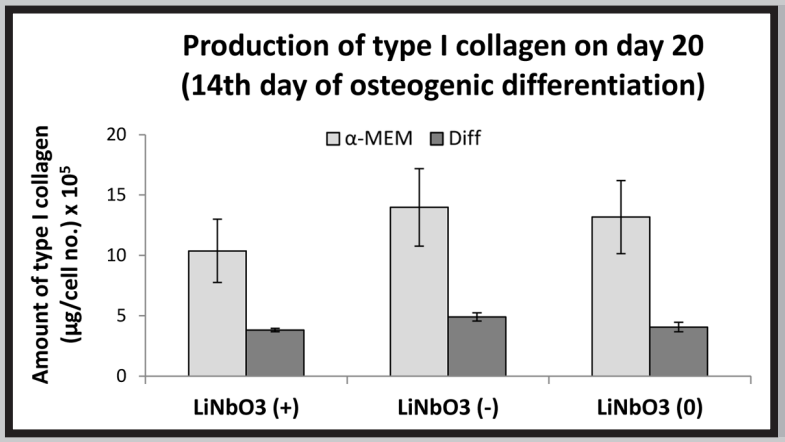

FIG. 3. Production of type I collagen per cell in human bone marrow mesenchymal stem cells in 20 day-old cultures on positively charged (+), negatively charged (-) and uncharged (0) $LiNbO_3$ surfaces. For the last 14 days, the cells were cultured in standard medium (α-MEM) or osteogenic medium (Diff). Mean ± S.D. from four measurements obtained from two samples for each experimental group.

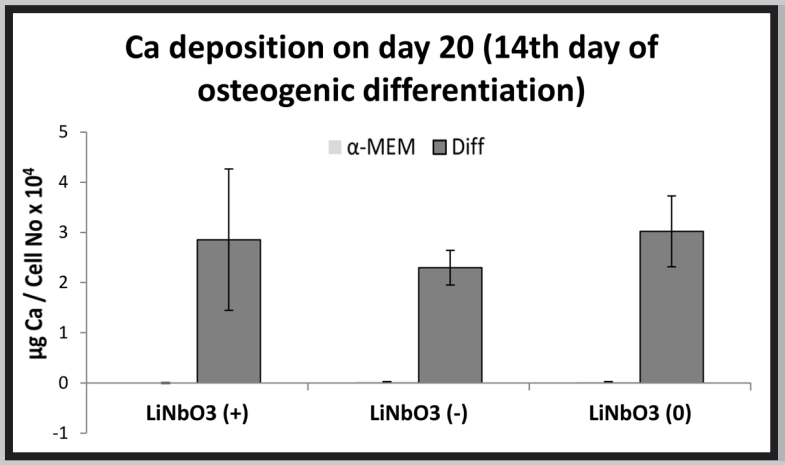

FIG. 4. Calcium deposition per cell in human bone marrow mesenchymal stem cells in 20 day-old cultures in standard medium (α-MEM) or osteogenic medium (Diff) on positively charged (+), negatively charged (-) and uncharged (0) $LiNbO_3$ surfaces. Mean ± S.D. from four measurements obtained from two samples for each experimental group.

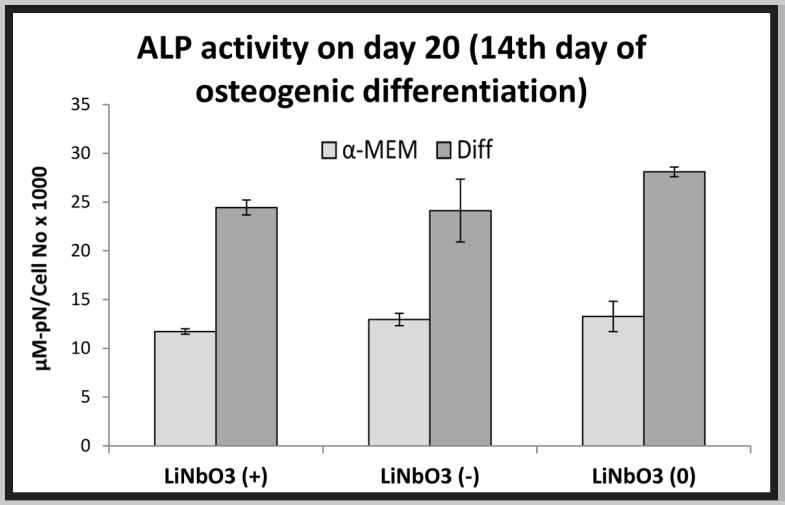

FIG. 5. Activity of alkaline phosphatase (ALP) per cell in human mesenchymal stem cells in 20 day-old cultures on positively charged (+), negatively charged (-) and uncharged (0) $LiNbO_3$ surfaces. For the last 14 days, the cells were cultured in standard medium (α-MEM) or osteogenic medium (Diff). Mean ± S.D. from four measurements obtained from two samples for each experimental group.

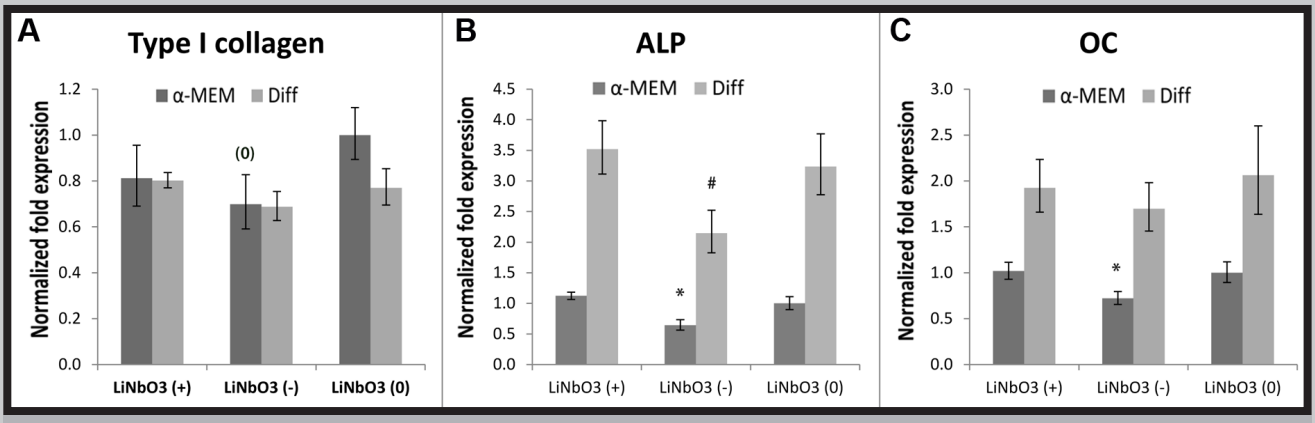

FIG. 6. Gene expression of type I collagen, alkaline phosphatase (ALP) and osteocalcin (OC) in 20 day-old cultures on positively charged (+), negatively charged (-) and uncharged (0) $LiNbO_3$ surfaces. For the last 14 days, the cells were cultured in standard medium (α-MEM) or osteogenic medium (Diff). Mean ± S.D. from 4 measurements for each experimental group. Statistical significance: * in comparison with the corresponding samples in α-MEM, # in comparison with the corresponding samples in osteogenic medium, and (0) in comparison with uncharged $LiNbO_3$ sample in α-MEM.

However, type I collagen was produced in higher amount by cells in the standard growth medium (α-MEM) than in osteogenic medium (FIG. 3). This result was surprising, because a higher production of type I collagen, considered as an early marker of osteogenic cell differentiation, can be expected in the osteogenic medium rather than in standard growth medium. An explanation might be that our method of collagen extraction was less successful in the case of cells in osteogenic medium, in which the extracellular matrix was strongly mineralized after 20 days of cultivation (14 days in osteogenic medium), as indicated by the markedly increased content of Ca^{2+} ions in comparison with the cultures in standard growth medium. In the latter cultures, the presence of Ca^{2+} ions was practically non-measurable (FIG. 4). In addition, the expression of type I collagen at the mRNA level was similar in cells cultures in both standard and osteogenic medium (see below). No significant differences in collagen production and matrix mineralization were found on the surfaces with different polarization (FIGs. 3 and 4).

The activity of alkaline phosphatase (ALP), i.e. an enzyme participating in bone matrix mineralization, considered as a medium-term marker of osteogenic cell differentiation, was significantly higher in cells grown for 14 days in the differentiation medium than in cells in the standard growth α-MEM medium. However, no differences in the ALP activity were observed in cells among the tested samples with different polarization (FIG. 5).

The evaluation of osteogenic markers at mRNA expression level revealed some significant differences among the cells cultured on the $LiNbO_3$ with various surface polarization. The cells on negatively-charged surfaces expressed in the standard growth medium expressed a significantly lower amount of type I collagen mRNA than the cells on non-charged $LiNbO_3$ (FIG. 6 A). The expression of mRNA for ALP was lower on negatively charged surfaces than on positively-charged and non-charged surfaces, which was apparent in both standard α-MEM and osteogenic media (FIG. 6 B). A similar trend was also found in the case of expression of osteocalcin, a late marker of osteogenic cell differentiation. The lowest expression of osteocalcin was found on negatively-charged surfaces in standard α-MEM (FIG. 6 C). Similar results were obtained in a study performed on gold nanoparticles with various surface functionalization. Positively charged Au nanoparticles (functionalized with amine groups) showed a higher cellular uptake, while negatively charged Au nanoparticles (functionalized with carboxyl groups) markedly reduced the ALP activity and calcium deposition in human bone marrow-derived mesenchymal stem cells [12].

The composition of the culture medium (i.e., standard growth α-MEM medium compared to osteogenic medium) did not significantly influence the expression of type I collagen (FIG. 6 A). However, the expression of ALP and osteocalcin was significantly increased in the medium with osteogenic factors (FIG. 6 B, C). The osteogenic medium might even mask the differences in the osteocalcin mRNA expression on materials with various polarization (FIG. 6 C).

Conclusions

The surface charge of $LiNbO_3$ due to ferroelectric polarization had no significant impact on the number, spreading, metabolic activity, production of type I collagen and activity of alkaline phosphatase in human bone marrow mesenchymal stem cells. However, the expression of osteogenic markers alkaline phosphatase and osteocalcin was higher in cells on positively-charged than on negatively-charged surfaces. The expression of type I collagen did not differ significantly between the positively and negatively-charged surfaces; however, on the negatively-charged surfaces, it was significantly lower than on the uncharged surfaces. In general, these results are in accordance with our earlier results obtained in human osteoblast-like Saos-2 cells on poled $LiNbO_3$ surfaces [11].

Acknowledgments

This study was supported by the Czech Science Foundation (grant No. 15-01558).

References

[1] Bacakova L., Filova E., Parizek M., Ruml T., Svorcik V.: Modulation of cell adhesion, proliferation and differentiation on materials designed for body implants. Biotechnol Adv 29 (2011) 739-767.
[2] Bacakova L., Filova E., Liskova J., Kopova I., Vandrovcova M., Havlikova J.: Nanostructured materials as substrates for the adhesion, growth, and osteogenic differentiation of bone cells. In: Nanobiomaterials in Hard Tissue Engineering. Applications of Nanobiomaterials. Volume 4, Ed. A. M. Grumezescu, Elsevier Inc., William Andrew Publishing, Oxford, Cambridge, 2016; pp. 103-153, ISBN 978-0-323-42862-0.
[3] Schneider G.B., English A., Abraham M., Zaharias R., Stanford C., Keller J.: The effect of hydrogel charge density on cell attachment. Biomaterials 25 (2004) 3023-3028.
[4] Kuwabara A., Hori N., Sawada T., Hoshi N., Watazu A., Kimoto K.: Enhanced biological responses of a hydroxyapatite/TiO_2 hybrid structure when surface electric charge is controlled using radiofrequency sputtering. Dent Mater J 31 (2012) 368-376.
[5] Tarafder S., Bodhak S., Bandyopadhyay A., Bose S.: Effect of electrical polarization and composition of biphasic calcium phosphates on early stage osteoblast interactions. J Biomed Mater Res B Appl Biomater 97 (2011) 306-314.
[6] Nakamura S., Kobayashi T, Yamashita K. Numerical osteobonding evaluation of electrically polarized hydroxyapatite ceramics. J Biomed Mater Res A 68 (2004) 90-94.
[7] Gao W, Feng B., Lu X., Wang J., Qu S., Weng J.: Characterization and cell behavior of titanium surfaces with PLL/DNA modification via a layer-by-layer technique. J Biomed Mater Res A 100 (2012) 2176-2185.
[8] Wolf-Brandstetter C., Hempel U., Clyens S., Gandhi A.A., Korostynska O., Oswald S., Tofail S.A., Theilgaard N., Wiesmann H.P., Scharnweber D.: The impact of heat treatment on interactions of contact-poled biphasic calcium phosphates with proteins and cells. Acta Biomater 8 (2012) 3468-3477.
[9] Jirka I., Vandrovcova M., Frank O., Tolde Z., Plšek J., Luxbacher T., Bacakova L., Stary V.: On the role of Nb-related sites of an oxidized β-TiNb alloy surface in its interaction with osteoblast-like MG-63 cells. Mater Sci Eng C Mater Biol Appl. 33(3) (2013) 1636-1645.
[10] Vandrovcova M., Jirka I., Novotna K., Lisa V., Frank O., Kolska Z., Stary V., Bacakova L.: Interaction of human osteoblast-like Saos-2 and MG-63 cells with thermally oxidized surfaces of a titanium--niobium alloy. PLoS One 9 (2014) e100475.
[11] Vanek P., Kolska Z., Luxbacher T., García J.A.L., Lehocky M., Vandrovcova M., Bacakova L., Petzelt J.: Electrical activity of ferroelectric biomaterials and its effects on the adhesion, growth and enzymatic activity of human osteoblast-like cells. J Phys D: Appl Phys 49 (2016) 175403.
[12] Li J.J., Kawazoe N., Chen G.: Gold nanoparticles with different charge and moiety induce differential cell response on mesenchymal stem cell osteogenesis. Biomaterials 54 (2015) 226-236.

PLASMA OXIDIZED Ti6Al4V AND Ti6Al7Nb ALLOYS FOR BIOMEDICAL APPLICATIONS

Bartosz Pązik[1], Jacek Grabarczyk[1]*, Damian Batory[1], Witold Kaczorowski[1], Barbara Burnat[2], Małgorzata Czerniak-Reczulska[1], Marcin Makówka[1], Piotr Niedzielski[1]

[1] Institute of Materials Science and Engineering, Lodz University of Technology, 1/15 Stefanowskiego St. 90-924 Lodz, Poland
[2] Department of Inorganic and Analytical Chemistry, University of Lodz, 12 Tamka St., Lodz, Poland
*e-mail: jacek.grabarczyk@p.lodz.pl

Abstract

Titanium and its alloys are one of the most popular metallic materials used in medicine for many years. Their favorable mechanical properties, high corrosion resistance and good biotolerance in an environment of tissues and body fluids, cause that they are widely used as construction material of orthopaedic dental and neurological implants. Their disadvantages are poor tribological properties manifested by high coeffi-cient of friction, scuffing and tendency to formation of adhesive couplings. In many research centers the works on improving the unfavorable tribological properties of titanium alloys are conducted. They rely on the use of modern methods of surface treatment including the thermo-chemical methods (nitriding, carburizing, oxidation) and the synthesis of thin films using PVD and CVD methods. In the presented work the glow discharge oxidation was applied to improve the surface properties of two-phase Ti6Al4V and Ti6Al7Nb titanium alloys. The results include a description of the obtained structure of the surface layer, surface topography, micro-hardness, wear ratio and corrosion resistance. The obtained results indicate changes in the surface layer of the material. The surface hardness was more than doubled and the depth of increased hardness region was up to 85 microns. This, in turn, several times decreased the wear rate of the modified materials while reducing the wear rate of the countersample. At the same time the carried out thermo-chemical treatment did not cause any structural changes in the core material. The oxidation process preferably influenced the corrosion properties of titanium alloys. Both, significant increase in the corrosion potential (approx. 0.36 V), as well as increased polarization resistance were observed. The modified surfaces also retained a high resistance to pitting corrosion.

Keywords: *titanium alloys, plasma oxidizing, tribology, wear, corrosion*

[Engineering of Biomaterials 135 (2016) 8-12]

Introduction

Titanium and its alloys due to the unique physical and chemical properties become more widely used in various industries, including aerospace, automotive, energy, ship-building, chemical and food industries as well as in medicine [1,2]. This is due to the small weight, high mechanical strength and Young's modulus twice lower in comparison to steel. Titanium alloys are characterized by the highest relative strength of all metallic materials up to a temperature of 600°C [2-4]. Covered by a thin oxide layer, mainly TiO_2, are resistant to atmospheric agents, sea water and many chemicals [5]. A number of characteristics of titanium in particular its alloys, makes them widely used in medicine for the production of medical instruments and implants. This is mainly due to the high relative strength, good corrosion resistance (in particular to physiological fluids and certain medications), high biocompatibility and ability to osseointegration. Titanium alloys have a relatively low Young's modulus of all metallic materials used for implants, which is the most similar to the one of the bone. Therefore they are most often used for pins of prostheses and acetabulum clamps. They are also used for dental and various spinal implants [4,6-8].

Based on the literature reports, among others Refs. [13-15], a beneficial effect of the oxidation of titanium and its alloys on the improvement of their corrosion resistance was confirmed. This treatment helps to increase the thickness and integrity of the oxide layer, which protects against corrosive agents. The most common methods for the oxidation of titanium alloys include an oxidation in fluidized bed, gas and plasma techniques [8,15]. In Refs. [14,16,17] the effect of oxidation in a fluidized bed on the properties of titanium is presented. In all cases, the thicknesses of the obtained layers were very small, not exceeding 10 μm. However, even such a thin layer enriched with oxygen helped to improve the tribological properties. In works [18-21] the effect of glow discharge oxidation on the tribological and mechanical properties of titanium alloys, primarily Ti6Al7Nb and Ti6Al4V, is presented. In each work the carried out oxidation process allowed a significant increase in hardness. The thickness of the obtained layers was greater than in the case of oxidation in a fluidized bed, ranging from 30 to about 105 μm for the plasma oxidation at a temperature of 850°C and time of 3 h [18]. Nowadays there are many works presenting the oxidation process as a hardening treatment, of which the main task is to improve the mechanical and tribological properties of the substrate. The difficulties encountered during the processes of oxidation of titanium and its alloys include very thin diffusion range and possible brittleness of the resulting layers, which excludes the modified material from its further application.

Materials and Methods

The tested materials were two-phase titanium alloys: Ti6Al4V and Ti6Al7Nb, in the form of samples cut from the rod. The chemical composition of the alloys was in line with ISO 5832-2 (Ti6Al4V) and ISO 5832-11 (Ti6Al7Nb) standards. The differences in the microstructure of the two materials in the initial state (FIG. 1) result from different thermal treatments which were applied at the stage of production. Both alloys were annealed at 750°C. Ti6Al7Nb alloy was annealed for a period of 75 min and cooled in air, whereas Ti6Al4V alloy was annealed for a period of 120 min and cooled with the furnace.

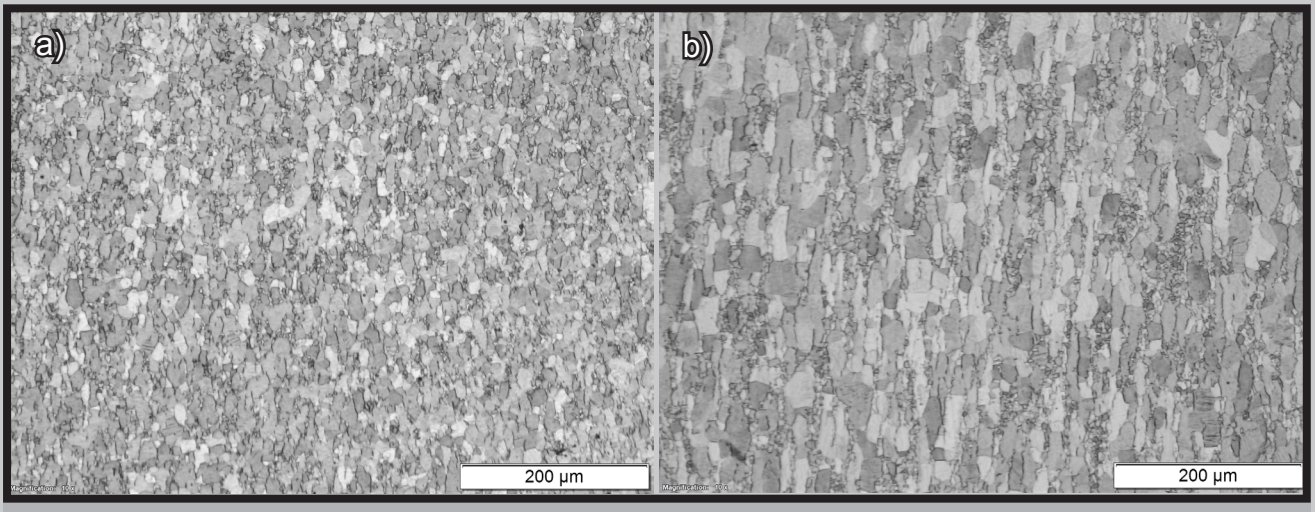

FIG. 1. Optical microscope images of initial microstructure of the titanium alloys: a) Ti6Al4V and b) Ti6Al7Nb.

The samples were grinded and mirror polished using colloidal silica suspension. Before the oxidation process the substrates were ultrasonically cleaned in acetone bath for 10 min and dried using a compressed air.

The process of diffusion strengthening by interstitial oxygen atoms was conducted in Ar/O_2 plasma. The samples were mounted on W electrode and placed in a quartz tube of the vacuum furnace. The annealing was conducted in a DC pulsed glow discharge in Ar atmosphere and pressure of 9 Pa. The plasma parameters during the whole process were kept at the same level: U = 850-1000 V and I = 50-60 mA. As soon as the temperature reached 900°C oxygen was introduced into the chamber at constant flow ratio O_2/Ar equal to 1/6. Oxygen was supplied for 60 s and then it was cut and the discharge took place only in an atmosphere of argon for 10 min. A total of 20 cycles were conducted to obtain the oxidized surface layers. After the process the batch was slowly cooled down with the furnace in continuous glow discharge in argon.

Microstructural examination was carried out using scanning electron microscope JEOL JSM-6610LV. Before the observation the prepared cross sections were etched by Kroll's reagent (1.5 ml of HF, 4 ml of HNO_3, 94 ml of H_2O). The roughness measurements were made with use of HOMMEL TESTER profilometer. The roughness parameters were examined before and after the plasma oxidation procedure.

The hardness distribution on the cross section profile was obtained for load of 100 g. with use of the Knoop indenter. The distance between the particular indentations was 10 µm.

Tribological parameters (coefficient of friction (CoF) and resistance against wear) were determined using ball on disc method. The investigations were performed under load of 10 N with the sliding speed 0.1 m/s on a distance of 1000 m. As the counterpart ¼ inch ZrO_2 ball was used. The tests were performed under temperature of 20 ±1°C and relative humidity of 50 ±2%. After the tests both, the wear tracks on the samples and wear scars on the countersamples were measured and used to determine their wear rates. For each sample and countersample four measurements were registered and the results were averaged.

Corrosion measurements were carried out using PGSTAT 302N potentiostat with NOVA 1.11 software. The measurements were performed in a thermostated electrochemical vessel in PBS (Phosphate Buffered Saline) solution at 37°C. Before the measurement electrolyte solution was deoxygenated with argon for 30 min. An active surface of samples was approx. 0.785 cm^2. The reference electrode was a saturated calomel electrode (E = 0.236 V_{SHE}), and the auxiliary electrode was a platinum gauze. Corrosion tests were carried out using electrochemical methods. The corrosion potential E_{cor} was measured in an open circuit (OCP) while recording the potential of the sample relative to the reference electrode for 1800 s. The value of polarization resistance, R_p, was determined according to Stern–Geary method in a scanning range of ± 20 mV vs. E_{cor} potential at the rate of 0.3 mV/s. Potentiodynamic characteristics were measured in a wide range of anodic polarization starting at potential E_{cor} – 0.2 V to 4 V with the scan rate of 1 mV/s.

Results and Discussion

After the oxidation processes significant changes in the surface layer of titanium alloys can be observed (FIG. 2). The subsurface layer of α-Ti, stabilized by the diffusion of oxygen, is visible. Next appears the oxygen diffusion zone which is a mixture α-Ti and β-Ti grains with the predominance of the former. The microstructure of vanadium containing alloy appears to be more fine-grained, especially in the case of the α-Ti regions.

For both modified materials a noticeable strengthening of the subsurface regions can be observed. The obtained hardness values compared to the unmodified materials are more than twice. With increasing distance from the surface the hardness decreases rapidly (FIG. 3). Based on both, the hardness distribution on the cross-section and SEM examinations the thickness of oxygen diffusion zone was estimated. In the case of all modified substrates its range was c.a. 85 µm which is in agreement with results presented in works [18-21].

After the oxidation procedure the coefficient of friction negatively increased for both modified alloys. Note, that prior to the ball on disc tests the plasma oxidized samples were polished to remove the top surface porous oxide layer. The initial value of CoF for Ti6Al4V alloy was 0.45, whereas for Ti6Al7Nb it was 0.46. The plasma oxidation process increased the values of CoF up to 0.72 and 0.74, respectively. As stated earlier in order to obtain the low roughness of the analyzed alloys, close to the one prior to oxidation process, both alloys were mirror polished. The polishing procedure made it possible to remove the outer layer of oxides, negatively influencing the surface topography, and, at the same time, not to affect the strengthening effect of the plasma treatment. Roughness parameters of Ti6Al4V and Ti6Al7Nb alloys before and after the plasma oxidation are presented in TABLE 1.

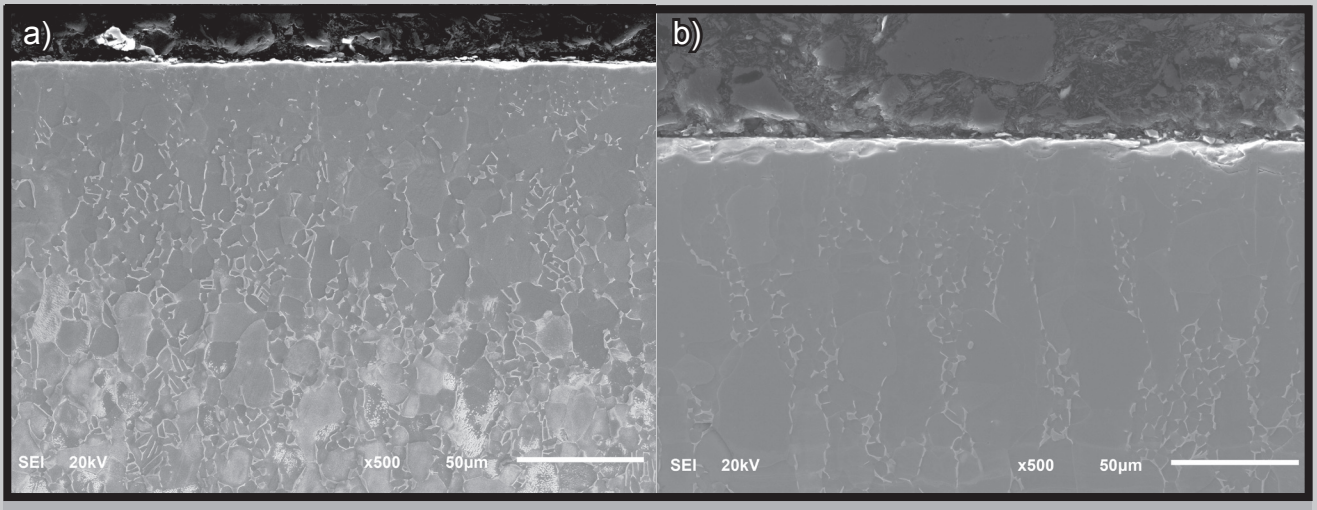

FIG. 2. SEM images of the microstructure after the plasma oxidation of: a) Ti6Al4V and b) Ti6Al7Nb.

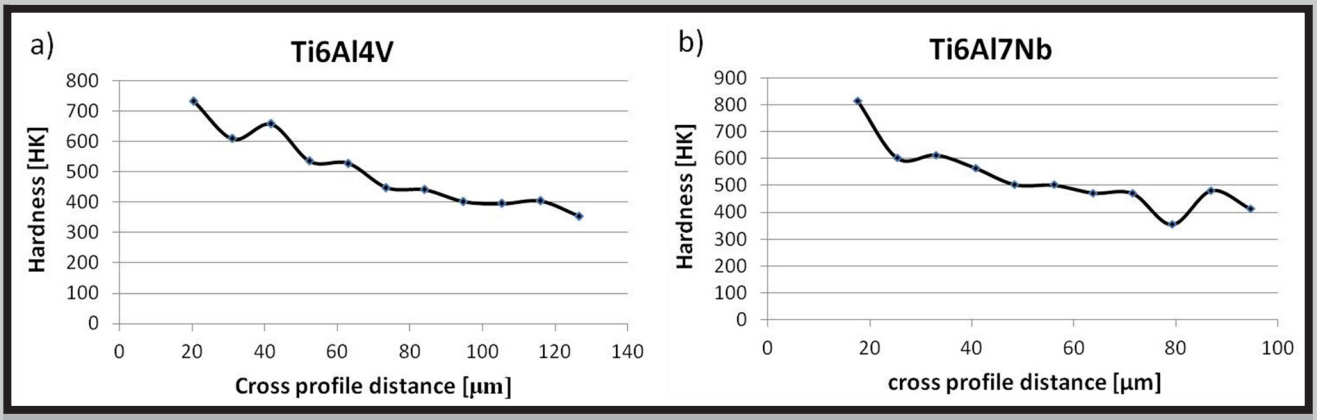

FIG. 3. Hardness distribution on the cross-section of the oxidized samples: a) Ti6Al4V and b) Ti6Al7Nb. The hardness is presented with respect to the distance from the surface of the sample.

TABLE 1. Roughness parameters of Ti6Al4V and Ti6Al7Nb alloys before and after the plasma oxidation.

Modification	Ti6Al4V				Ti6Al7Nb			
	Roughness parameters				Roughness parameters			
	Ra	Rp	Rz	Rmax	Ra	Rp	Rz	Rmax
Before	0.02	0.14	0.23	0.37	0.02	0.12	0.19	0.36
After oxidation	0.08	0.75	1.22	1.38	0.08	0.71	1.15	1.39
After oxidation and polishing	0.02	0.06	0.11	0.13	0.03	0.09	0.19	0.23

The wear rate (FIG. 4a) after the plasma oxidation was $0.171 \cdot 10^{-4}$ mm^3/Nm for Ti6Al4V alloy, which is one order of magnitude lower in comparison to the wear rate of unmodified sample. In the case of the Ti6Al7Nb alloy the wear rate after the plasma oxidation decreased seven times, giving the result $0.260 \cdot 10^{-4}$ mm^3/Nm. Also, the wear rate of the ceramic countersample (FIG. 4b) was significantly reduced. The obtained values of $0.066 \cdot 10^{-4}$ mm^3/Nm for the Ti6Al4V alloy, and $0.061 \cdot 10^{-4}$ mm^3/Nm for the Ti6Al7Nb alloy gave almost three times less wear rate of zirconium oxide countersample. The effect of reducing the wear rates during the tribological tests was obtained despite the fact that the coefficient of friction for both alloys noticeably deteriorated. This may be explained by the increased hardness of the surface and hence higher abrasion resistance. We did not observe the brittleness of the surface layer possibly caused by the oxidation process. The wear tracks were uniform and the values of CoF were stable and did not change during the entire test. The thickness of the modified surface layer (approx. 85 µm) has been found to be sufficient for bearing the applied load during the test.

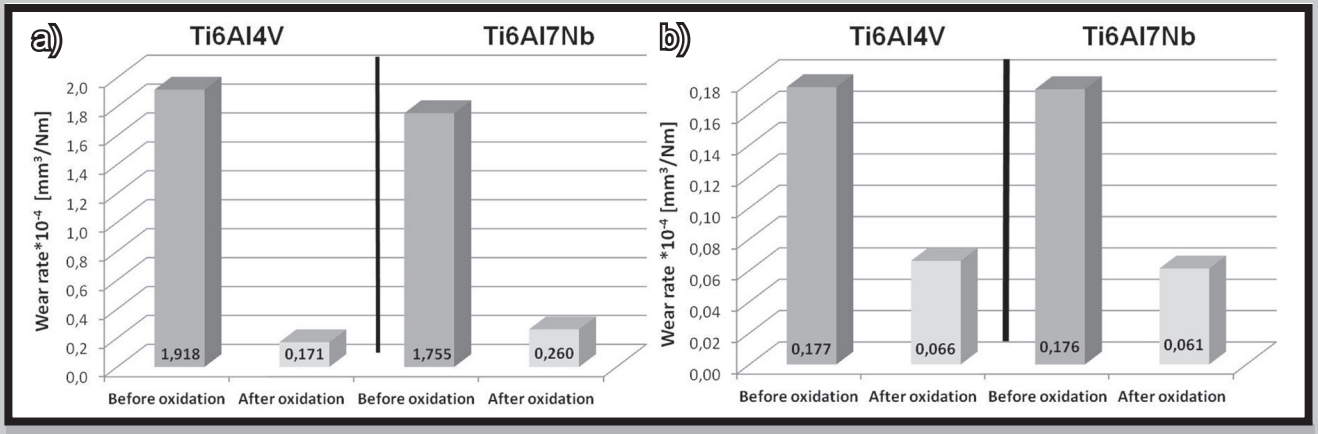

FIG. 4. Wear rates before and after the plasma oxidation of: a) Ti6Al4V and Ti6Al7Nb alloys, b) ZrO_2 countersamples.

TABLE 2. Corrosion parameters of the analyzed alloys.

Sample	E_{cor} (V)	R_p (MΩ cm²)	CR (μm/year)
Ti6Al4V before oxidation	-0.410 ±0.039	0.46 ±0.21	0.71 ±0.34
Ti6Al4V after oxidation	-0.049 ±0.021	1.25 ±0.20	0.22 ±0.03
Ti6Al7Nb before oxidation	-0.395 ±0.041	0.23 ±0.03	1.15 ±0.15
Ti6Al7Nb after oxidation	-0.021 ±0.054	2.35 ±0.15	0.11 ±0.01

Based on the corrosion studies the characteristic parameters characterizing the corrosion properties of the titanium alloys were calculated. The resulting mean values of E_{cor}, R_p and CR along with the standard deviations calculated from measurements of a series of three samples from each type are shown in TABLE 2.

Based on the values of corrosion parameters it can be seen that both titanium alloys have a similar resistance to corrosion - corrosion potential, polarization resistance and corrosion rate have a similar values, and any differences are within the measurement error. The plasma oxidation process resulted in a significant increase in the corrosion potential (approx. 0.36 V). The increase in the polarization resistance - approx. 3 times for the Ti6Al4V alloy, and approx. one order of magnitude for the Ti6Al7Nb alloy, was also observed. Higher polarization resistance provides a better corrosion resistance of the tested materials, which is also confirmed by the values of the corrosion rate presented in TABLE 2. In both cases, the corrosion rate of the modified alloys is lower and therefore it can be concluded, that the plasma oxidation procedure increased the corrosion resistance of studied alloys, wherein the observed effect was greater in the case of niobium containing Ti alloy.

In FIG. 5 the potentiodynamic characteristics of the tested alloys, which can be used to evaluate their resistance to pitting corrosion are presented. The characteristics obtained for titanium alloys prior to the surface modification are typical of passive materials, but differ in the course depending on the alloy. In both cases, at the potential of approx. 0 V begins a passive low-current range of the potentiodynamic characteristics (passive current density of 5-6 μA/cm²), and depending on the alloy it has a different width. The passive range of the Ti6Al4V alloy is very wide, and it ends at a potential of approx. 3 V. In the case of the Ti6Al7Nb alloy its range is narrower and ends just at a potential approx. 1.2 V. The observed increase in the corrosion current at higher potentials is associated with the processes of electrochemical oxidation of the titanium alloys surface. It was also confirmed by microscopic observations of the surface, performed after the polarization processes (data not shown here), which revealed the presence of corrosion damage. In contrast, the potentiodynamic characteristics of titanium alloys registered after the oxidation processes have a shape almost identical within the entire range of polarization. In both cases the Tafel's range of the characteristic is shifted towards higher potential values, and lower corrosion currents, whereas the further course of the characteristic is also typical for samples in the passive state. In any case, a sharp increase in current associated with pitting corrosion did not occur. The lack of the corrosion damage was also confirmed by the microscopic analysis of the surface.

To summarize, the performed examinations have shown, that the plasma oxidation allows the positive influence on the corrosion resistance of the analyzed alloys.

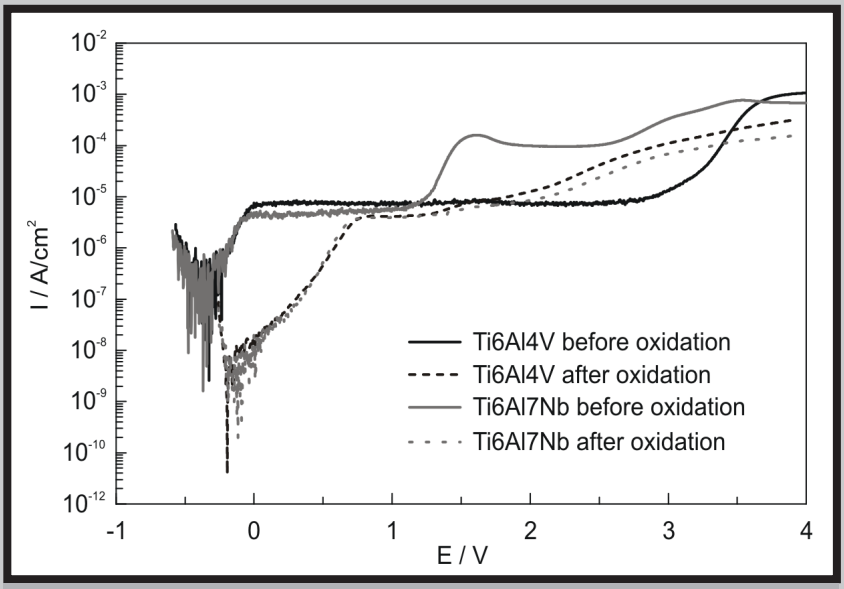

FIG. 5. Potentiodynamic characteristics of the investigated titanium alloys.

Conclusions

The conducted processes of diffusion strengthening of titanium alloys by interstitial oxygen atoms positively influenced the investigated properties. We managed to increase twice the hardness of the surface of the tested alloys and the thickness of the diffusion zone was estimated to be approx. 85 μm. These parameters resulted in a reduction of the wear rate determined in ball on disc tests. The registered value of the wear rate of the Ti6Al4V alloy decreased by one order of magnitude, whereas for the Ti6Al7Nb alloy it was 7 times lower. The lower values of wear rate were achieved despite the fact, that the friction coefficients, compared to the unmodified alloys, have increased from 0.45 to 0.7. The plasma oxidation of Ti alloys favourably affected their corrosion resistance. The value of the corrosion potential significantly increased (approx. 0.36 V). At the same time the polarization resistance increased three times for the Ti6Al4V alloy and 10 times for the Ti6Al7Nb alloy, which demonstrates the better corrosion resistance of the modified samples. The results of the potentiodynamic studies also confirmed a high resistance of the modified alloys against the pitting corrosion. As a drawback of the process of oxidation an increase in surface roughness can be pointed out. It results in the need of additional polishing treatment restoring the original surface smoothness and removing a thin surface layer of a porous oxide.

In summary, it can be stated that the plasma oxidation of titanium alloys favourably influenced the tribological and corrosion properties of both Ti6Al4V and Ti6Al7Nb alloys.

Acknowledgment

This work has been supported by the National Centre for Research and Development under grant "Load bearing capacity tribological junctions for biomedical applications", PBS3/A5/44/2015

References

[1] Gierzyńska-Dolna M., Lijewski M.: Zastosowanie tytanu i jego stopów w implantologii i inżynierii biomedycznej. Inżynieria Materiałowa 4 (2012) 315-318.
[2] Adamus J.: Perspektywy zastosowania tytanu w nowoczesnych konstrukcjach budowlanych. Inżynieria Materiałowa 4 (2012) 319-323.
[3] Adamus J.: Tytan i jego stopy jako materiał stosowany na elementy tłoczne. Inżynieria Materiałowa 5 (2009) 310-313.
[4] Adamus J.: Gierzyńska-Dolna M.: Tytan współczesnym materiałem stosowanym na implanty. Inżynieria Materiałowa 3 (2012) 189-192.
[5] Dobrzański L.A.: Metaloznawstwo opisowe, Wydawnictwo Politechniki Śląskiej, Gliwice 2013.
[6] Michnik J.: Biomateriały w chirurgii kostnej, Wydawnictwo Politechniki Śląskiej, Gliwice 1992.
[7] Jedynak B., Mierzwińska-Nastalska E.: Tytan – właściwości i zastosowanie w protetyce stomatologicznej. Dental Forum 1 (2013) 75-78.
[8] Bylica A., Sieniawski J.: Tytan i jego stopy, Państwowe Wydawnictwo Naukowe, Warszawa 1985.
[9] Michalik R.: Wpływ obróbki cieplnej na odporność korozyjną stopów na implanty długotrwałe. Inżynieria Materiałowa 3 (2005) 135-138.
[10] Kubiak K., Sieniawski J.: Podstawy obróbki cieplnej dwufazowych stopów tytanu. Zeszyty Naukowe Politechniki Opolskiej, Seria Mechanika z. 58, 250 (1999) 83-91.
[11] Gierzyńska-Dolna M., Sobociński M.: Wpływ obróbki powierzchniowej na własności tribologiczne stopów tytanu. Zeszyty Naukowe Politechniki Opolskiej, Seria Mechanika z. 58, 250 (1999) 21-26.
[12] Hepner M.: Metody modyfikacji warstwy wierzchniej tytanu i jego stopów w aspekcie własności tribologicznych. Zeszyty Naukowe Politechniki Opolskiej, Seria Mechanika z. 88, 318 (2006) 273-276.
[13] Bloyce A., Qi P.-Y., Dong H., Bell T.: Surface modification of titanium alloys for combined improvements in corrosion and wear resistance. Surface and Coatings Technology 107 (1998) 125-132.
[14] Aniołek K., Kupka M., Barylski A.: Sliding wear resistance of oxide layers formed on a titanium surface during thermal oxidation. Wear 356-357 (2016) 23-29.
[15] Zhecheva A., Sha W., Malinov S., Long A.: Enhancing the microstructure and properties of titanium alloys through nitriding and other surface engineering methods. Surface & Coatings Technology 200 (2005) 2192-2207.
[16] Lubas M., Podsiad P., Jasiński J., Jasiński J., Sitarz M.: Właściwości tribologiczne tytanu po procesie utleniania w złożu fluidalnym. Inżynieria Materiałowa 5 (2014) 393-396.
[17] Rylski A., Mendzik K., Jasiński J.: Badania powłoki tlenkowej powstającej na tytanie po utlenianiu w złożu fluidalnym. Inżynieria Materiałowa 5 (2006) 1197-1199.
[18] Januszewicz B., Wendler B., Liśkiewicz T., Kaczmarek Ł.: Struktura i twardość stopu tytanu Ti6Al4V po obróbce utwardzającej utlenianiem. Inżynieria Materiałowa 5 (2005) 454-456.
[19] Wang S., Liao Z., Liu Y., Liu W.: Influence of thermal oxidation temperature on the microstructural and tribological behavior of Ti6Al4V alloy. Surface & Coatings Technology 240 (2014) 470-477.
[20] Lieblicha M., Barriusoa S., Multignera M., Gonzalez-Doncela G., Gonzalez-Carrasco J.L.: Thermal oxidation of medical Ti6Al4V blasted with ceramic particles: Effects on the microstructure, residual stresses and mechanical properties, Journal of The Mechanical Behavior of Biomedical Materials 54 (2016) 173-184.
[21] Luo Y., Chen W., Tian M., Teng S.: Thermal oxidation of Ti6Al4V alloy and its biotribological properties under serum lubrication. Tribology International 89 (2015) 67-71.

THE INFLUENCE OF DIFFERENT TYPES OF CARBON NANOMATERIAL ON THE PROPERTIES OF COATINGS OBTAINED BY EPD PROCESS

Alicja Wedel-Grzenda, Karolina Tran, Aneta Frączek-Szczypta*

AGH University of Science and Technology,
Faculty of Materials Science and Ceramics,
Department of Biomaterials,
Al. Mickiewicza 30, 30-059 Krakow, Poland
*e-mail: afraczek@agh.edu.pl

Abstract

The first part of research is concentrated on the examination of four kinds of carbon nanomaterials: graphene oxide (GO), multi-walled carbon nanotubes (MWCNT), multi-walled carbon nanotubes functionalized by authors in acids mixture (MWCNT-F) and multi-walled carbon nanotubes with hydroxyl groups (MWCNT-OH). Their microstructure was observed in transmission electron microscopy (TEM). Based on these microphotographs, the diameters of carbon nanotubes were measured. Then, in order to determine the chemical composition of GO, MWCNT-F and MWCNT-OH, X-ray photoelectron spectroscopy was applied. The second part of study concerns the properties of the coatings deposited electrophoretically on titanium surface from previously examined nanomaterials. The coatings from individual nanomaterials, as well as hybrid layers (combination of two kinds of nanomaterial: graphene oxide with one of the nanotubes' type) were deposited. Microstructure of the coatings was evaluated with the use of scanning electron microscopy (SEM). Furthermore, surface properties, important while considering usage of these materials in biological applications: wettability and surface free energy were evaluated. These materials are meant for application in regeneration and stimulation of nerve cells. All the research carried out so far indicate the influence of nanotubes' functionalization degree on the properties of their suspension, as well as the characteristics of the deposited coating. It also influences the interaction between two types of nanomaterials. Functionalization in strong acids introduces functional groups which change nanotubes' dimensions, properties and behavior in solution.

Keywords: *graphene oxide, multi-walled carbon nanotubes, electrophoretic deposition, hybrid coatings, surface properties, microstructure*

[Engineering of Biomaterials 135 (2016) 13-20]

Introduction

Material's surface properties have a significant meaning while considering interactions between the material and its surroundings. Especially in the field of biomedicine, where biomaterials are used to repair, replace or stimulate the tissue, material's surface is an important factor that determines the behavior of the implant in living tissues and biological environment response on the material [1]. For example, in the case of metallic implants, surface roughness influences the fixation of implant in bone and it can improve the response of bone tissue [2]. But not only surface topography, but also chemistry of implants has a great meaning for the cells response [3]. For metallic implants one of the important factors is also the modification of their surface for improvement of anti-corrosion properties in biological environment. In the literature there are a lot of examples of surface modification [4]. One way is to coat the surface with a layer of different materials. Coatings protect metallic surface from corrosion and improve wear properties, as well as inhibit the release of ions into tissues [1]. In biological applications, metals are often used for orthopedic and dental implants. One often uses metallic implant for hard tissue reconstruction is titanium and its alloys. Despite the fact that titanium is a material with a high biocompatibility, thanks to the possibility of naturally self-passivation in a body fluid there is still a need to modify the surface in order to improve e.g. their bioactivity. One method for improving the bioactivity is covering its surface with bioactive material, which leads to a better bond with bone. Often ceramics (hydroxyapatite) [4,5] or glass-ceramics (bioglass) [6] coatings on metals are created. Moreover, the examples of hybrid ceramic – non-ceramics coatings can be found [1]. Not only bioactivity coatings are used, but also other coatings that mimic natural extracellular matrix, or the conductive coatings are used in particular for the regeneration of the nervous tissue cells. In the case of conductive coatings, their properties can induce nerve cells for better growth, proliferation and creating networks. Among the materials which have both conductive properties and perfectly mimic the extracellular matrix of neural tissue are carbon nanotubes [7-9]. There are many methods to apply the coatings on metal surface, one of which is electrophoretic deposition technique (EPD). EPD is a method, which allows for obtaining thin coatings on conducting surfaces. It is a technique, in which an electric field is applied to move the charged particles which then become deposited on the conducting substrate, rinsed in particles' solution [10]. This method is very popular due to the simple equipment needed, short deposition time, possibility of modification for particular application. What is more, layers can be deposited on a substrate of any shape [11]. In literature, there are examples of application of this method to carbon nanomaterials. Chunsheng et al. [12] prepared multi-walled carbon nanotubes films by cathodic EPD. They examined the influence of solvent composition on the microstructure and properties of coating. They noticed that the resistance of deposited films increased, because of the hydrogen evolution and its adsorption on nanotubes. As a solution, they suggested using anodic EPD. This kind of EPD was earlier applied by different research teams [13,14]. They deposited functionalized multi-walled carbon nanotubes on stainless steel and titanium from three kinds of suspensions and proved that the suspension influences structure and properties of obtained coatings. Park [15] deposited graphene oxide (GO) from water suspension on carbon steel in order to create an anti-corrosion coating. They did not obtain satisfactory results for the GO layer alone, but this layer turned out to be well enough as an underlying coating, then coated with the organic coating. Earlier, Singh et al. [16] obtained uniform, anti-corrosion composite layers from graphene oxide and polymeric isocyanate matrix. Ultrathin coatings with the thickness of 40 nm did not have any cracks.

Quite new issue comprises creation of hybrid nanocomposite layers, for example connection of nanotubes and graphene oxide. Wang et al. [17] prepared carbon nanotubes-graphene oxide electrodes by layer by layer self-assembly technique on copper foils. This kind of material can be used as an energy storage device in microsystems. They obtained homogenous coatings, in which the amount of energy stored is controlled by the thickness of the coating. Zhang et al. [18] produced similar layers, in which the synergy between two nanocarbon phases improved wear and lowered a friction coefficient of DLC surfaces under applied load and vacuum conditions. These two examples show the possible usage of such hybrids in technical applications. Formerly, the connection of nanotubes and pure, not oxidized graphene is presented in the literature for such applications [19,20]. But the novel approach is to use these nanomaterials to create coatings on materials intended for biomedical purposes. These hybrids can be created not only by layer by layer method, but also by depositing a mixture of these two types of carbon nanomaterials.

In this work we compare the properties of coatings, deposited from various types of carbon nanomaterials, as well as the hybrids of these materials on titanium surfaces. The examination allows for better understanding of the influence of different types of carbon nanomaterials on coating's properties such as microstructure, morphology, surface energy and wettability important in terms of potential application of these materials in regeneration and stimulation of nerve cells.

Materials and Methods

Materials

All nanomaterials were produced by Nanostructured & Amorphous Materials, Inc. (USA). Unmodified multi-walled carbon nanotubes (MWCNT) with diameters above 50 nm and lengths from 10 to 20 μm dissolved in isopropanol were used. Then, multi-walled carbon nanotubes with hydroxyl groups, MWCNT-OH, which had diameters in range of 10 to 20 nm and lengths between 0.5-2 μm, according to manufacturer were also applied. Multi-walled carbon nanotubes, denoted as MWCNT-F were functionalized by the authors in the mixture of concentrated acids H_2SO_4 and HNO_3 in the proportion of 3:1. This procedure, applicable for various types of carbon nanotubes is described in the literature [21,22]. It allows to remove the residues of metallic catalysts and introduce functional groups on the nanotubes' surface [22]. Moreover, graphene oxide (GO) with thickness from 0.55 to 1.2 nm and the diameter from 0.5 to 3 μm was also in this investigation. Then, from three types of nanomaterials, the suspensions were prepared as shown in the scheme (FIG. 1). The percentage ratio of ethanol to acetone to water was: 62% to 21% to 17%, respectively. Mixtures of GO, MWCNT-OH and MWCNT-F in this solution were called GO+m, MWCNT+m and MWCNT-F+m, respectively.

In the next step, the chosen kinds of suspensions were mixed together in different volume ratios (MWCNT-OH to GO and MWCNT-F to GO). The aim was to deposit in the subsequent step hybrid nanomaterials' coatings.

All coatings were deposited onto titanium Grade 2 (Ti: 99.6%, Fe:0.3%, O:0.25%, N:0.03%, C:0.08%, H:0.013% (wt%)) surfaces, which had the form of flat, rectangular plates, 1 cm x 2 cm. Before deposition, the Ti surfaces were prepared in four steps. Firstly metal substrates were rinsed in acetone for 30 min with the use of ultrasonic bath (Polsonic, Sonic 05). Then the same step was repeated in ethanol. After drying in ambient conditions the plates were etched in 5% hydrofluoric acid solution (Chempur) for 1 min. The etched titanium plates were finally rinsed with distilled water, to remove acid residues.

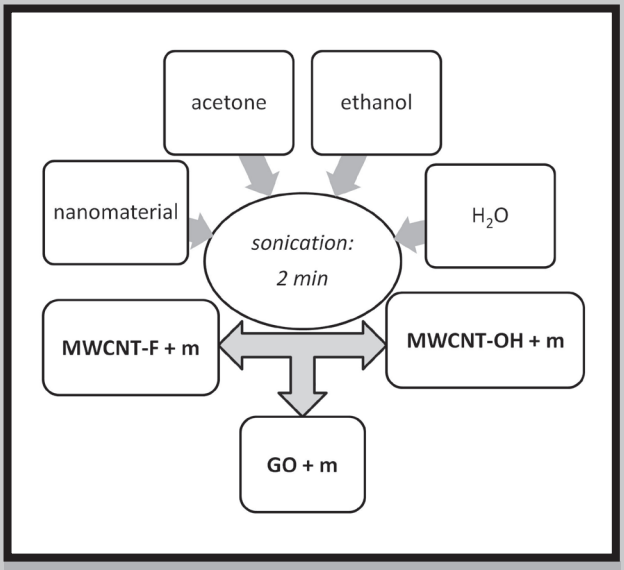

FIG. 1. Preparation of the nanomaterials' suspensions in the mixture of ethanol, acetone and water.

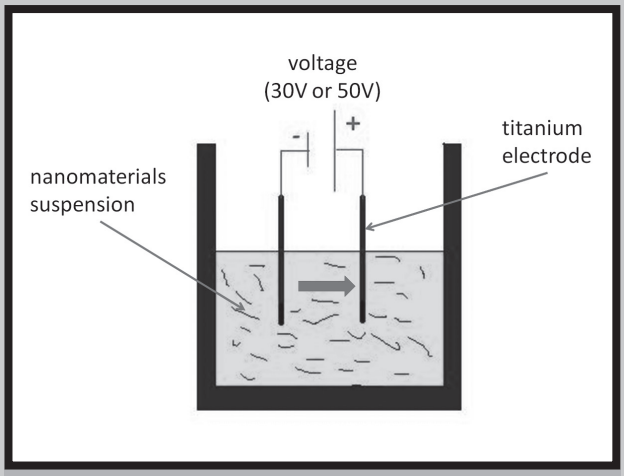

FIG. 2. The scheme of EPD method.

Methods

The electrophoretic deposition process (EPD) was performed on the apparatus built in Department of Biomaterials. The scheme of this method is presented in FIG. 2. The system consists of two electrodes. One of them is the titanium surface, on which the coating is deposited. Here it worked as an anode, as the carbon nanoparticles in all suspensions were negatively charged (due to the presence of carboxyl and hydroxyl groups) and they migrated into the positively charged titanium surface. Also titanium was used as a cathode. The distance between the electrodes was about 1 cm. The voltages of deposition were 30 V and 50 V, depending on the deposited material. The deposition times were in range from 10 s to 30 s. After deposition, all coatings were dried in ambient conditions.

In order to observe the morphology and microstructure of the nanomaterials (GO, MWCNT, MWCNT-F and MWCNT-OH) transmission electron microscopy (TEM, JEOL JEM-1011, Japan) was applied. Additionally, on the basis of obtained microphotographs the diameters of three types of carbon nanotubes were measured using ImageJ software.

The absolute Zeta potential (ζ) of all carbon nanomaterials was performed in EAW solution using combination of electrophoresis and the LDV technique (Laser Doppler Velocimetry , Malvern Zetasizer Nano ZS), with the laser light source of wavelength λ = 520 nm.

The second part of research is connected with the examination of the coatings, deposited on titanium surfaces.

Scanning electron microscopy (SEM, Nova NanoSEM 200, FEI) was applied for observations of the deposited coatings' microstructure. Microphotographs were obtained at a 100 000 x magnification, which allowed to observe the surface in nanoscale. The cross sections of the selected coating deposited on Ti substrates and thin foils for STEM observations were performed using Focused Ion Beam technique (FIB/SEM Hitachi NB5000, 40 kV). To investigate the internal structure of the selected coating High Resolution Scanning Transmission Electron Microscopy (STEM Hitachi HD 2700, 200 kV, Cs corrected) was employed.

The chemical composition of GO, MWCNT-F and MWCNT-OH was investigated by X-ray photoelectron spectroscopy (XPS - Vacuum Systems Workshop Ltd., England) method. Depth of analysis was about 5 nm. Mg Ka X-ray radiation with 200 W energy was used as the excitation source. Electron energy analyzer was set to FAT mode with pass energy 22 eV. The absolute content of carbon (C1s) and oxygen (O1s) was determined. Additionally, for MWCNT-OH sample the absolute content of the nitrogen (N1s) was also detected.

The surface wettability was measured with the sessile drop method. The drop shape analysis (DSA 10Mk2, Kruss, Germany) system, connected with the computer software was applied to analyze the contact angle and the shape of the drops. About 0.2 µL volume drops of distilled water were put on the surface of each sample; several measurements for one sample were performed. As a reference sample, the surface of etched titanium was used.

The surface energy of the coatings was calculated with the Owens-Wendt method. The method is based on measuring the contact angle of polar liquid – water and the non-polar liquid – diiodomethane. The surface tensions of these two liquids are known. The values of dispersive energy and polar energy are for water: γ_d = 21.8 mJ/m^2 and γ_p = 51 mJ/m^2; respectively, and for diiodomethane: γ_d = 48.5 mJ/m^2 and γ_p = 2.3 mJ/m^2; respectively. Then, on the basis of these measurements for two liquids, the surface energy with its components was calculated using computer software, connected with the drop shape analysis system.

Results and Discussions

Morphology and microstructure of carbon nanomaterials

TEM microphotographs of graphene oxide (GO) is presented below (FIG. 3). Using this method the typical microstructure of layered graphene is observed. In this magnification, several layers of graphene can be observed. The manufacturer's data suggest that the number of graphene oxide layers can reach up to 10. The graphene oxide is single or few layers of graphene obtained after exfoliation of graphite oxide in water using sonication. The main difference between graphite oxide and graphene oxide is, thus, the number of layers. Graphite oxide is a compound of carbon, oxygen, and hydrogen in variable ratios, obtained by treating graphite with strong oxidizers.

TEM microphotographs of CNTs indicate meaningful differences in the length of nanotubes. Functionalized nanotubes (MWCNT-F) are significantly shorter than unfunctionalized ones (MWCNT). The most probable reason is that they were cut during the functionalization procedure. This process usually influences the size of nanotubes – the closed ends of nanotubes, produced e.g. in CVD process, become open after functionalization, which is also connected with the decrease of their lengths [22,23].

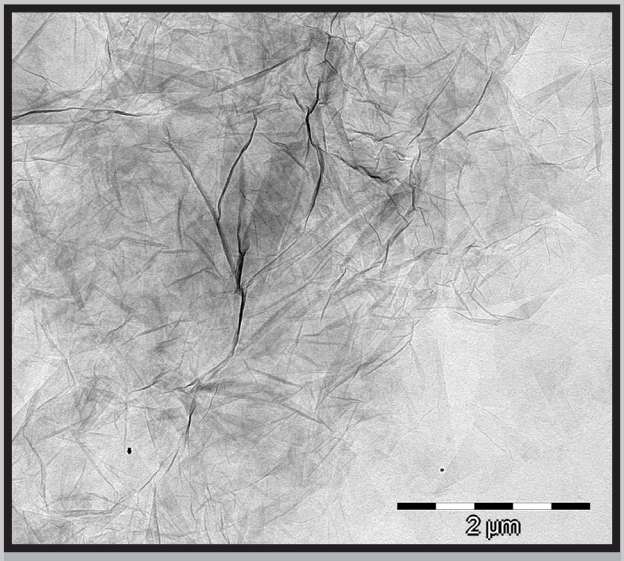

FIG. 3. TEM microphotograph of graphene oxide (GO).

What is more, they are less bundled – functional groups, introduced on their surfaces reduce van der Waals interactions between individual nanotubes and - as a consequence - decrease their tendency to agglomeration [24]. Similar effect was observed for commercial nanotubes with hydroxyl groups (MWCNT-OH), but here the nanotubes' lengths seem to be bigger. The method of MWCNT-OH functionalization is not known but analyzing amount of functional groups on their surface using XPS reveals that this amount is lower (described further) which suggests that the conditions of the oxidation process were milder. Therefore, they did not have such a large impact on the destruction of the structure of graphene layers in the nanotubes (FIG. 4). TEM micrographs show that the structure of all analyzed nanotubes was disturbed as evidenced by the reduction in diameter along the length of nanotubes and numerous folds of graphene layers.

The fact that functionalized nanotubes have lower agglomeration tendency has a great meaning when they are used in a form of suspension for electrophoretic deposition. After functionalization, they are able to form stable suspensions with controlled dispersion [23]. It is known that the stability of suspension is an important factor for successful deposition.

The average diameters of carbon nanotubes are presented in FIG. 5. For all types of nanotubes, they were similar, in range from 20 to 40 nm. The smallest diameters were measured for functionalized nanotubes (MWCNT-F), but they are within the error range for all types. The measurements confirm that the process of functionalization changes the length of nanotubes, rather than their diameters.

All types of nanomaterials (GO, MWCNT, MWCNT-F and MWCNT-OH) were deposited using EPD technique. In such a way four types of coatings were obtained. Also, three types of hybrid coatings: GO in connection with MWCNT-OHs (in two volume ratios, 1:1 and 5:1) and GO with MWCNT-Fs (in volume ratio 5:1) were obtained. All the deposited coatings are presented in TABLE 1. Preparation of stable dispersed carbon nanomaterials suspension in a mixture of solvents is the essential stage preceding the EPD process. The most popular strategy is the production of an electrostatically stabilized dispersion, which in general terms, requires the preparation of a solvent medium in which the particles have a high ζ-potential, while keeping the ionic conductivity of the suspensions low [25].

FIG. 4. TEM microphotographs of MWCNT (A), MWCNT-F (B) and MWCNT-OH (C).

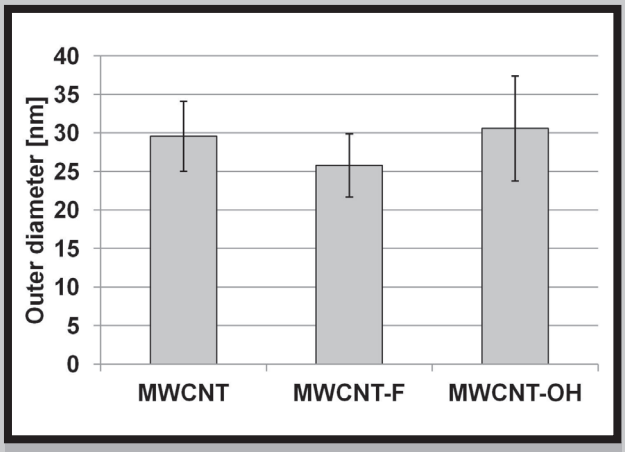

FIG. 5. Average outer diameters of all three types of carbon nanotubes.

According to standard for Zeta potential for colloids in water [26], if the absolute value of ζ is smaller than ±25 mV, the repulsive force is not strong enough to overcome the van der Waals attraction between the particles, and hence the particles begin to agglomerate [27]. The stability of carbon nanomaterial suspensions in mixture of ethanol, acetone and water has been determined by ζ-potential measurements (TABLE 1). For all solutions the ζ-potential was at the level of -20 mV. This value is below -25 mV, but stability of all analyzed suspensions was high and EPD process was stable for all suspensions. The difference may be due to the assumed value of viscosity of a solution consisting of three solvents and viscosity values are very crucial parameters for calculation of Zeta potential. For mixture of ethanol, acetone and water the viscosity was estimated based on the procedure proposed by Song S. et al. [28]. Moreover, the contractual value ±25 mV of ζ-potential is checked for aqueous solutions but in the case of mixtures of solvents, this value may be different.

Because the conditions of the EPD process, such as voltage and time depend upon the suspension but do not affect the surface properties of the obtained coatings, thus they were not described in detail for each coating. The concentration of each pure carbon nanomaterial in suspensions (GO, MWCNT, MWCNT-F and MWCNT-OH) is 2.9 mg/ml.

TABLE 1. Compositions of the carbon nanomaterials coatings and Zeta potential of the solutions containing carbon nanomaterials.

Sample	GO (m)	MWCNT (isopropanol)	MWCNT-F (m)	MWCNT-OH (m)	Volume ratio	Zeta potential [mV]
Ti	Reference sample: titanium surface etched in 5% HF (Ti-HF)					
GO	X				-	-19.9
MWCNT		X			-	-
MWCNT-F			X		-	-22.6
MWCNT-OH				X	-	-16.2
GO:MWCNT-OH 1:1	X			X	1:1	-23.0
GO:MWCNT-OH 5:1	X			X	5:1	-20.4
GO:MWCNT-F1:1	X		X		5:1	-23.5

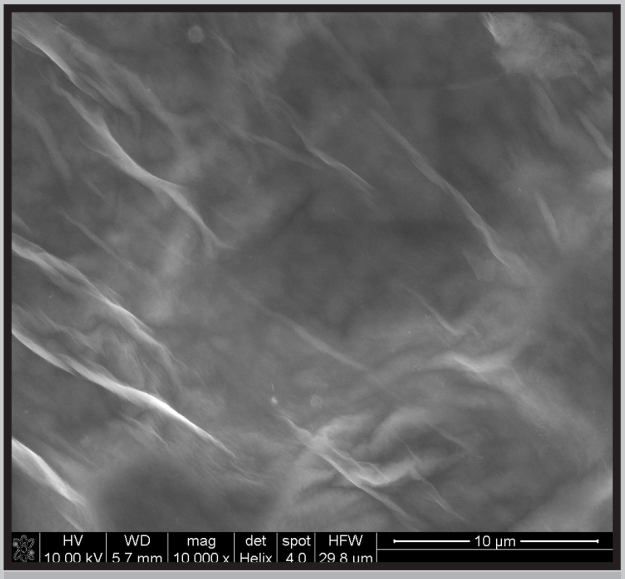

FIG. 6. SEM microphotograph of GO; magnification 10 000x.

Morphology and microstructure of carbon nanomaterial coatings

Microstructure and morphology of pure and hybrid coatings on Ti surface were analyzed using SEM. SEM microphotograph of GO coatings is shown in FIG. 6. Morphology of this material is typical. In the microphotograph a thin coating of graphene oxide covering the metal surface and reproducing its topography is observed. Only visible trails on the metal surface indicate the presence of graphene layers on its surface.

FIG. 7 shows microphotographs of the deposited coatings of MWCNT, MWCNT-OH and MWCNT-F. The coating of functionalized nanotubes (MWCNT-F, FIG. 7B) seems to be the more dense and homogenous than the other two types of coatings, especially MWCNT-OH. The MWCNT-OH is irregularly spread on the plate, partly parallel and partly perpendicular to the surface and even porous-like structure was observed in this surface (FIG. 7C). Similar nanotubes' tendency was observed in our previous work but for different metal substrate (stainless steel) and deposited solution [14]. This behavior, in particular for MWCNT-Fs can be explained by that during the EPD process metal hydroxides at the electrode surface can be formed which favours creation of hydrogen bonds between the metallic plate and oxidized nanotubes. Moreover, good homogeneity of MWCNT-F coatings is assured by the stability of the suspension, which was used for deposition. It can be then deduced that the level of functionalization not only influences the behavior of nanotubes in suspension, but also has an impact on the properties of coating, deposited from this suspension. The coating of unfunctionalized nanotubes (MWCNT) is homogenous but less dense in comparison with MWCNT-F coating; more space between singular tubes can be observed. Not very compact structure as for MWCNT and MWCNT-OH coatings may be interesting substrate type for cell culture, allowing the transport of nutrients and waste products.

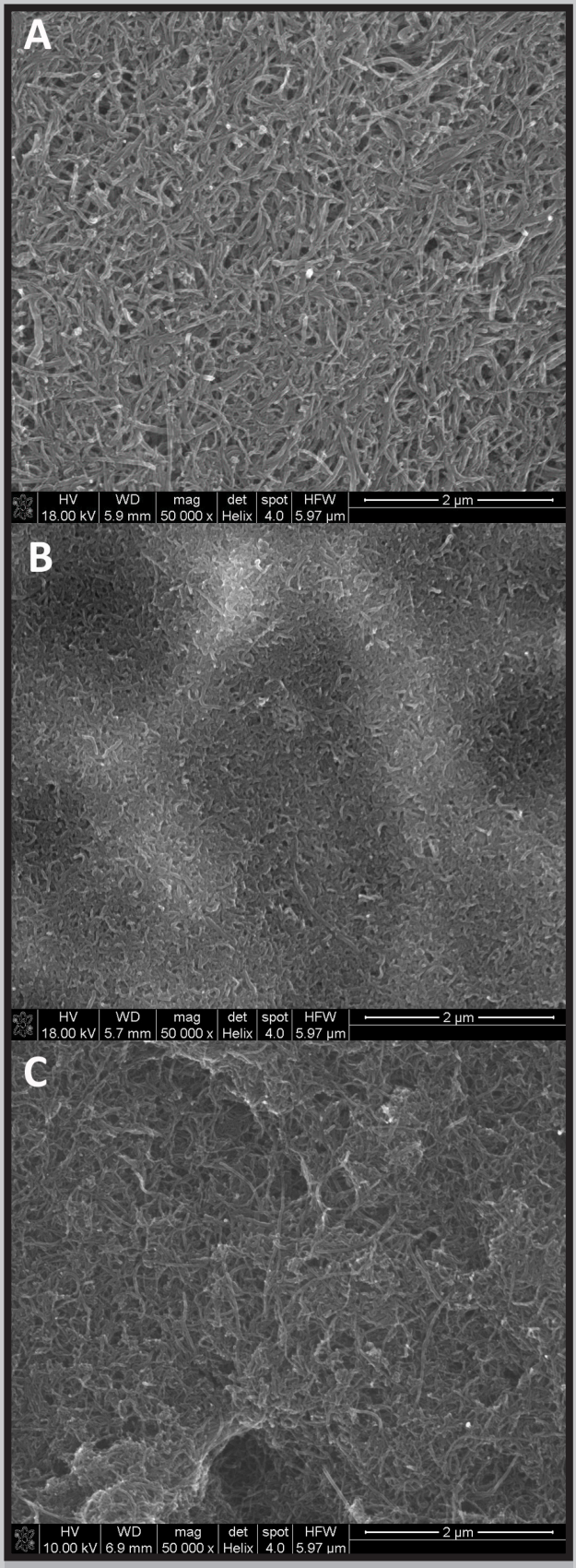

FIG. 7. SEM microphotographs of MWCNT (A), MWCNT-F (B) and MWCNT-OH (C); magnifications 50 000x.

Topography and microstructure of hybrid coatings is presented in FIG. 8 A, B, C. A lot of tangled nanotubes can be observed on the surface, when the coating consists of MWCNT-OH and GO in the same proportions. Generally, the morphology of this sample was not significantly different than for pure MWCNT-OH (FIG. 7 C). When concentration of graphene oxide in solution was higher than nanotubes' concentration (FIG. 8 B), the MWCNT-OH seems to be covered with the GO and the surface is smoother. Similar situation can be observed in the case when the coating contains 5 times more GO than MWCNT-F (FIG. 8 C). But here the nanotubes are more agglomerated and tangled than on FIG. 8 B. It can be deduced that the topography of final coating depends on the types of nanomaterials, their proportions and deposition conditions. It can be also connected with another surface properties – depending on the fact, how much nanotubes are on the surface and how they influence the continuous layer of graphene oxide.

Surface chemistry of carbon nanomaterials coatings

XPS is a useful method of analyzing the surface chemistry of carbon nanomaterials. The absolute content of carbon (C1s), oxygen (O1s) and nitrogen (N1s) in all three nanomaterials is presented in TABLE 2. XPS analysis confirmed high content of oxygen in GO. One of the advantages of the graphene oxide is its easy dispersability in water and other organic solvents, as well as in different matrices, due to the presence of the oxygen functionalities [29]. From this point of view, this type of nanomaterial is ideal for coatings' deposition by EPD method. Functionalized carbon nanotubes (MWCNT-F) have higher oxygen content and lower carbon content, when compared to commercially available nanotubes (MWCNT-OH). It suggests that MWCNT-Fs are more hydrophilic and their structure is more defected than the structure of MWCNT-OH, but they have more functional groups. Moreover, a significant difference between coatings was observed due to the presence of the peak located at around 532.9 eV, which corresponds to functionalized oxygen-containing groups, such as carboxylate, hydroxyl, quinone and lactone [30,31]. The oxygen atomic content for this peak deduced from XPS analysis of GO was over twice as high (77.7%) as compared to MWCNT-F and MWCNT-OH (36.35% and 34.59%, respectively), which confirms high content of functional groups on their surfaces.

TABLE 2. Chemical composition of nanomaterials.

Sample	Absolute content [%]		
	C	O	N
GO	69.06	30.94	-
MWCNT-F	83.99	16.01	-
MWCNT-OH	89.83	9.45	0.72

Average contact angles for all examined coatings are shown in FIG. 9. Only unfunctionalized carbon nanotubes coating (MWCNT) has smaller wettability than pure titanium. High hydrophobic character of pure MWCNT is typical for this type of materials and majority of carbon materials. Presence of the functional groups such as –COOH and –OH significantly decreases the hydrophobicity of carbon nanomaterials. The lowest contact angle was observed for MWCNT-F coating (θ = 25°). Also GO coatings possess high wettability (θ = 33°), which confirmed results obtained from XPS analysis (TABLE 1). Although, higher wettability was expected for GO than MWCNT-F coatings.

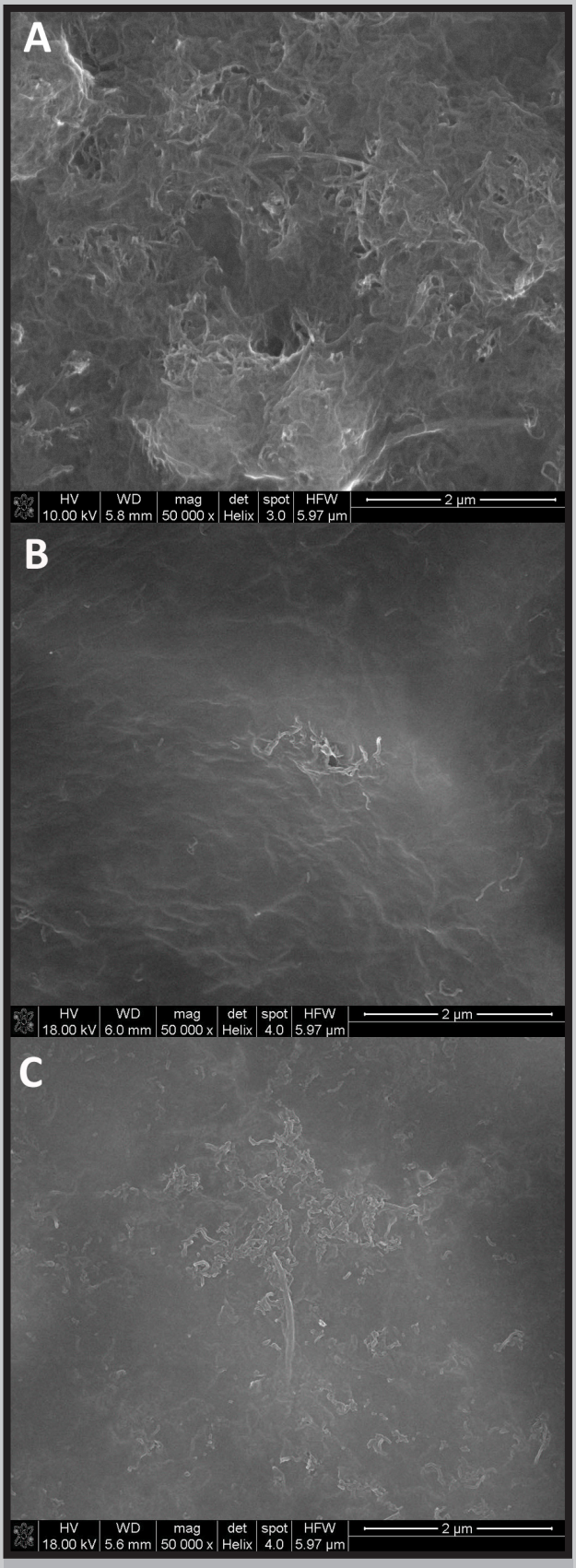

FIG. 8. SEM microphotographs of deposited hybrid layers: GO:MWCNT-OH 1:1 (A); GO:MWCNT-OH 5:1 (B) and GO:MWCNT-F 5:1 (C); magnifications 50 000x.

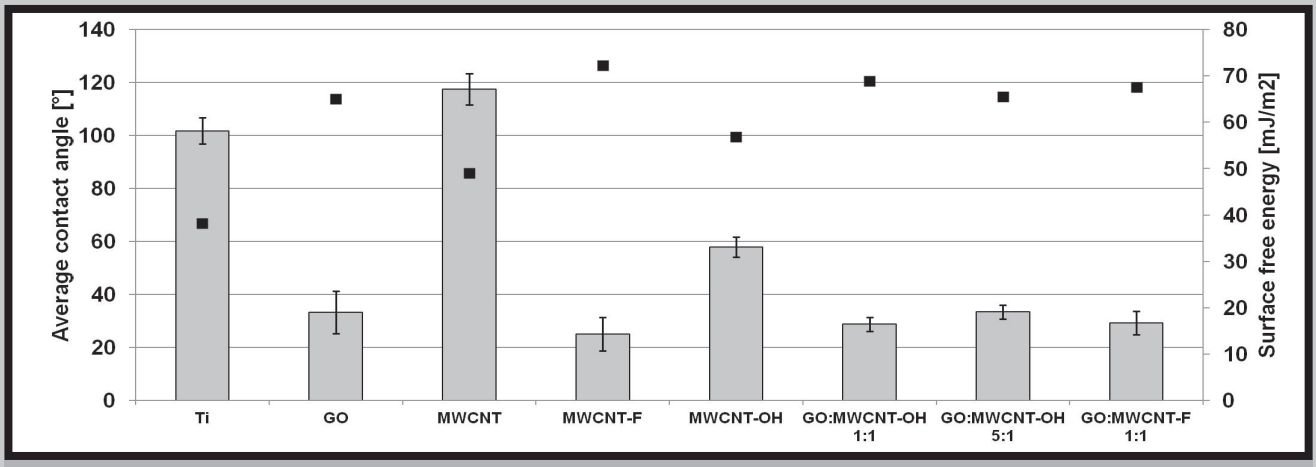

FIG. 9. Contact angles (bars) and average surface free energy (points) values for all deposited coatings.

These results can indicate the influence of the other factor on the wettability of these coatings, connected probably with different morphology of these surfaces. Comparing contact angle of MWCNT-F coating with the coating of commercially available carbon nanotubes (MWCNT-OH), the MWCNT-F coating is more hydrophilic. That is important regarding biological applications of this nanomaterial. After functionalization, nanotubes not only become biostable and harmless, but also give the opportunity of further modification, e.g. with proteins or growth factors, depending on the intended application. What is more, thanks to functionalization nanotubes become more soluble in organic solvents [32] which has a great meaning while using them in EPD process.

For hybrid coatings, it can be noticed that the average contact angle strongly depends on the presence of graphene oxide in the coating. This effect was observed especially for hybrid coatings containing both GO and MWCNT-OH. Regardless of the contribution of the MWCNT-OH in the coating, the wettability is significantly below this value for pure MWCNT-OH coating. One of the probable reasons for this is the presence of GO on the surface of hybrid coating. Presence of GO layer especially for GO:MWCNT-OH 5:1 and GO:MWCNT-F 5:1 is confirmed by SEM microphotographs (FIG. 8 B, C). Moreover, thanks to cross section of GO:MWCNT-OH 5:1, the observation of MWCNT-OH and GO arrangement inside the coating is possible using STEM. STEM microphotograph also confirmed the presence of graphene oxide in the upper layers of coating (FIG. 10).

Surface free energy for deposited coatings is related to their contact angle. So nanomaterials with oxygen groups are more hydrophilic and they have higher surface energy. This parameter is important in the case of interaction of biomaterial's surface with tissue. Titanium, bioinert in biological environment, has relatively low surface energy. All deposited coatings have higher surface energy than titanium which may indicate that the surface of these materials has more active sites capable to interact with cells [33]. Surface energy of implant material is one of the important factors in the process of cells adhesion [34]. Cell adhesion is one of the first steps essential to subsequent proliferation and differentiation of cells before tissue formation [35].

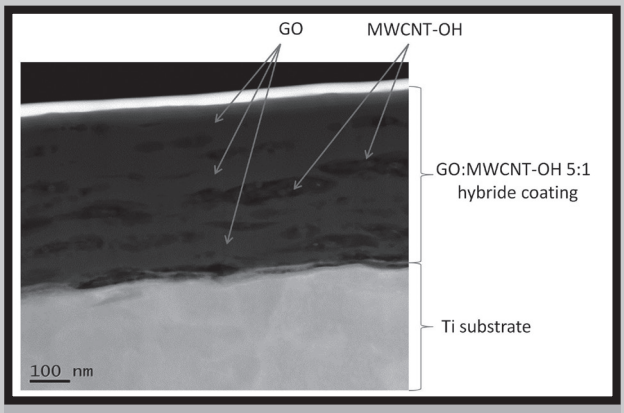

FIG. 10. Microphotograph STEM of GO:MWCNT-OH 5:1 hybrid coating on Ti substrate.

Conclusions

This study indicates that it is possible to obtain pure carbon nanomaterial and especially hybrid carbon nanomaterial coatings on Ti plates using EPD process. Preparation of these coatings is easy and fast and EPD method allows controlling the properties of the coatings, such as thickness, through the changing of the deposition process parameters. These results indicate that the microstructure and properties of final coating deposited on titanium is connected with the type of carbon nanomaterial and in particular - with the degree of functionalization. The functional groups on CNTs not only change the dimensional properties of nanotubes, but also influence their behavior in suspension, prepared for electrophoretic deposition. Thanks to these carboxyl and hydroxyl groups it is possible to obtain a stable suspension, and consequently homogenous coating. Microstructure of hybrid coatings depends on the carbon nanotubes to graphene oxide ratio. Due to the combination of carbon nanotubes and graphene oxide, different in terms of concentration of the functional groups and ratio of these two phases, it is possible to control the physicochemical properties of coatings, such as wettability and surface energy. These parameters and others, like surface morphology and roughness have a significant influence on cells adhesion and proliferation.

Acknowledgements

The work has been supported by the National Science Centre (Grant no: UMO-2013/11/D/ST8/03272).

References

[1] Catauro M., Papale F., Bollino F.: Characterization and biological properties of TiO_2/PCL hybrid layers prepared via sol-gel dip coating for surface modification of titanium implants. Journal of Non-Crystalline Solids 415 (2015) 9-15.
[2] Imade S., Mori R., Uchio Y., Furuya S.: Effect of implant surface roughness on bone fixation: the differences between bone and metal pegs. J Orthop Sci. 14(5) (2009) 652-657.
[3] Wong J.Y., Leach J.B., Brown X.Q.: Balance of chemistry, topography, and mechanics at the cell-biomaterial interface: Issues and challenges for assessing the role of substrate mechanics on cell response. Surface Science 570(1) (2004) 119-133.
[4] Hanawa T.: Biofunctionalization of titanium for dental implant. Japanese Dental Science Review 46(2) (2010) 93-101.
[5] De Lange G., Donath K.: Interface between bone tissue and implants of solid hydroxyapatite or hydroxyapatite-coated titanium implants. Biomaterials 10(2) (1989) 121-125.
[6] Pajamäki K., Lindholm T., Andersson Ö., Karlsson K., Vedel E., Yli-Urpo A., et al.: Bioactive glass and glass-ceramic-coated hip endoprosthesis: experimental study in rabbit. Journal of Materials Science: Materials in Medicine 6(1) (1995) 14-18.
[7] Fraczek-Szczypta A.: Carbon nanomaterials for nerve tissue stimulation and regeneration. Mater Sci Eng C Mater Biol Appl. 34 (2014) 35-49.
[8] Lee W., Parpura V.: Carbon nanotubes as substrates/scaffolds for neural cell growth. Progress in brain research 180 (2009) 110-125.
[9] Fabbro A., Prato M., Ballerini L.: Carbon nanotubes in neuroregeneration and repair. Adv Drug Deliv Rev. 65(15) (2013) 2034-2044.
[10] Boccaccini A., Keim S., Ma R., Li Y., Zhitomirsky I.: Electrophoretic deposition of biomaterials. Journal of The Royal Society Interface. The Royal Society 7(5) (2010) S581-S613.
[11] Besra L., Liu M.: A review on fundamentals and applications of electrophoretic deposition (EPD). Progress in materials science 52(1) (2007) 1-61.
[12] Du C., Heldbrant D., Pan N.: Preparation and preliminary property study of carbon nanotubes films by electrophoretic deposition. Materials Letters 57(2) (2002) 434-438.
[13] Benko A., Przekora A., Wesełucha-Birczyńska A., Nocuń M., Ginalska G., Błażewicz M.: Fabrication of multi-walled carbon nanotube layers with selected properties via electrophoretic deposition: physicochemical and biological characterization. Applied Physics A. 122(4) (2016) 1-13.
[14] Fraczek-Szczypta A., Dlugon E., Weselucha-Birczynska A., Nocun M., Blazewicz M.: Multi walled carbon nanotubes deposited on metal substrate using EPD technique. A spectroscopic study. Journal of Molecular Structure 1040 (2013) 238-245.
[15] Park J.H., Park J.M.: Electrophoretic deposition of graphene oxide on mild carbon steel for anti-corrosion application. Surface and Coatings Technology 254 (2014) 167-174.
[16] Singh B.P., Nayak S., Nanda K.K., Jena B.K., Bhattacharjee S., Besra L.: The production of a corrosion resistant graphene reinforced composite coating on copper by electrophoretic deposition. Carbon 61 (2013) 47-56.
[17] Wang S.-C., Yang J., Zhou X.-Y., Xie J., Ma L.-L., Huang B.: Electrochemical properties of carbon nanotube/graphene oxide hybrid electrodes fabricated via layer-by-layer self-assembly. Journal of Electroanalytical Chemistry 722 (2014) 141-147.
[18] Zhang L., Pu J., Wang L., Xue Q.: Synergistic Effect of Hybrid Carbon Nanotube-Graphene Oxide as Nanoadditive Enhancing the Frictional Properties of Ionic Liquids in High Vacuum. ACS applied materials & interfaces. ACS Publications 7(16) (2015) 8592-8600.
[19] Tung V.C., Chen L.-M., Allen M.J., Wassei J.K., Nelson K., Kaner R.B., et al.: Low-temperature solution processing of graphene- carbon nanotube hybrid materials for high-performance transparent conductors. Nano letters 9(5) (2009) 1949-1955.
[20] Yu D., Dai L.: Self-assembled graphene/carbon nanotube hybrid films for supercapacitors. The Journal of Physical Chemistry Letters 1(2) (2009) 467-470.
[21] Liu J., Rinzler A.G., Dai H., Hafner J.H., Bradley R.K., Boul P.J., et al.: Fullerene pipes. Science. American Association for the Advancement of Science 280(5367) (1998) 1253-1256.
[22] Fraczek-Szczypta A., Menaszek E., Blazewicz S.: Some observations on carbon nanotubes susceptibility to cell phagocytosis. Journal of Nanomaterials 2011 (2011) ID 473516, 1-8.
[23] Firme C.P., Bandaru P.R.: Toxicity issues in the application of carbon nanotubes to biological systems. Nanomedicine 6(2) (2010) 245-256.
[24] Balasubramanian K., Burghard M.: Chemically functionalized carbon nanotubes. Small. 1(2) (2005) 180-192.
[25] Hirata E., Uo M., Takita H., Akasaka T., Watari F., Yokoyama A.: Multiwalled carbon nanotube-coating of 3D collagen scaffolds for bone tissue engineering. Carbon 49(10) (2011) 3284-3291.
[26] Standard A., others.: Zeta potential of colloids in water and waste water. Am Soc Testing Mater. (1985) 4187-4182.
[27] Castro M., Al-Dahoudi N., Oliveira P., Schmidt H.: Multi-walled carbon nanotube-based transparent conductive layers deposited on polycarbonate substrate. Journal of Nanoparticle Research 11(4) (2009) 801-806.
[28] Song S., Peng C.: Viscosities of binary and ternary mixtures of water, alcohol, acetone, and hexane. Journal of Dispersion Science and Technology 29(10) (2008) 1367-1372.
[29] Graphenea [Internet]. Available from: http://www.graphenea.com/pages/graphene-oxide#.V2v0MPmLTIV
[30] Ohta T., Yamada M., Kuroda H.: X-ray photoelectron spectroscopy of p-benzoquinone, hydroquinone and their halogen--substituted derivatives. Bulletin of the Chemical Society of Japan 47(5) (1974) 1158-1161.
[31] Vigolo B., Hérold C., Marêché J.-F., Ghanbaja J., Gulas M., Le Normand F., et al.: A comprehensive scenario for commonly used purification procedures of arc-discharge as-produced single-walled carbon nanotubes. Carbon 48(4) (2010) 949-963.
[32] Tran P.A., Zhang L., Webster T.J.: Carbon nanofibers and carbon nanotubes in regenerative medicine. Adv Drug Deliv Rev. 61(12) (2009) 1097-1114.
[33] Liu X., Lim J.Y., Donahue H.J., Dhurjati R., Mastro A.M., Vogler E.A.: Influence of substratum surface chemistry/energy and topography on the human fetal osteoblastic cell line hFOB 1.19: phenotypic and genotypic responses observed in vitro. Biomaterials 28(31) (2007) 4535-4550.
[34] Gentleman M.M., Gentleman E.: The role of surface free energy in osteoblast-biomaterial interactions. International Materials Reviews 59(8) (2014) 417-429.
[35] Lai H.-C., Zhuang L.-F., Liu X., Wieland M., Zhang Z.-Y., Zhang Z.-Y.: The influence of surface energy on early adherent events of osteoblast on titanium substrates. J Biomed Mater Res A 93(1) (2010) 289-296.

GENOTOKSYCZNOŚĆ ANTYBAKTERYJNYCH BIOSZKIEŁ WYTWORZONYCH METODĄ ZOL-ŻEL WOBEC *SALMONELLA TYPHIMURIUM*

Piotr Jadczyk[1]*, Barbara Umińska-Wasiluk[1], Lidia Ciołek[2], Joanna Karaś[3], Andrzej Olszyna[3]

[1] Wydział Inżynierii Środowiska, Politechnika Wrocławska,
ul. Wybrzeże Wyspiańskiego 27, 50-370 Wrocław
[2] Zakład Technologii Ceramiki,
Instytut Ceramiki i Materiałów Budowlanych,
ul. Postępu 9, 02-676 Warszawa
[3] Wydział Inżynierii Materiałowej, Politechnika Warszawska,
ul. Wołoska 141, 02-507 Warszawa
*e-mail: piotr.jadczyk@pwr.edu.pl

Streszczenie

Problemem w stomatologii są choroby przyzębia. W zaawansowanej fazie tej choroby konieczna jest chirurgiczna interwencja z zastosowaniem odpowiednich biomateriałów dla regeneracji tkanek. Dlatego celem tej pracy było określenie genotoksyczności potencjalnych biomateriałów w postaci bioszkła glinokrzemianowego (B-I) oraz bioszkieł wapniowokrzemianowych (Z-5 i Z-8) wobec Salmonella typhimurium TA 98 i TA 100 w mikropłytkowym teście rewersji mutacji. Bioszkła ekstrahowano w 10 cm^3 dimetylosulfotlenku (DMSO), wytrząsając przy 250 rpm po 2 g bioszkieł B-I i Z-8 oraz 1 g bioszkła Z-5 przez 72 h w temperaturze 37°C. Ekstrakty bioszkieł wprowadzano do testu w postaci roztworów w DMSO. Rozcieńczano je połowicznie, tak aby w czasie ekspozycji uzyskać dawki bioszkieł B-I i Z-8: 0,25-8,0 mg/cm^3 a bioszkła Z-5: 0,125-8,0 mg/cm^3. Wykonano testy bez i z aktywacją metaboliczną 30% frakcją S9.

Bioszkło B-I powodowało rewersję mutacji w szczepie TA 100 w obecności frakcji S9. Pozwala to wnioskować, że bioszkle B-I występowały mutageny pośrednie powodujące powstawanie mutacji podstawiania par zasad na wykrywanie których pozwala szczep TA100. Dane literaturowe wskazują, że mogło to być następstwem łącznego działania składników tego bioszkła oraz pozostałości substratów użytych do ich wytworzenia. Nie zawierało ono mutagenów bezpośrednich powodujących powstawanie mutacji podstawiania par zasad ani mutagenów bezpośrednich i pośrednich powodujących powstawanie mutacji zmiany fazy odczytu, na wykrywanie których pozwala szczep TA98. Bioszkła Z-5 i Z-8 nie powodowały rewersji mutacji wobec żadnego ze stosowanych szczepów testowych.

Uzyskane wyniki pozwalają rekomendować bioszkła Z-5 i Z-8 do dalszych badań poprzedzających ich kliniczne zastosowanie. Bioszkło B-I nie powinno być stosowane w chirurgicznym leczeniu chorób przyzębia.

Słowa kluczowe: *bioszkło wapniowokrzemianowe, bioszkło glinokrzemianowe, biomateriał, test rewersji mutacji, mutagenność*

[Inżynieria Biomateriałów 135 (2016) 21-27]

GENOTOXICITY OF ANTIBACTERIAL BIOGLASSES OBTAINED BY SOL-GEL METHOD FOR *SALMONELLA TYPHIMURIUM*

Piotr Jadczyk[1]*, Barbara Umińska-Wasiluk[1], Lidia Ciołek[2], Joanna Karaś[3], Andrzej Olszyna[3]

[1] Faculty of Environmental Engineering,
Wrocław University of Science and Technology,
ul. Wybrzeże Wyspiańskiego 27, 50-370 Wrocław, Poland
[2] Department of Ceramic Technology,
Institute of Ceramics and Building Materials,
ul. Postępu 9, 02-676 Warszawa, Poland
[3] Faculty of Materials Science and Engineering,
Warsaw University of Technology,
Pl. Politechniki 1, 00-661 Warszawa, Poland
*e-mail: Piotr.jadczyk@pwr.edu.pl

Abstract

Periodontal disease causes problems in dentistry. Surgical intervention with appropriate biomaterials for tissue regeneration is necessary in advanced stages of the disease. Therefore, the aim of this study was to determine the genotoxicity of potential biomaterials in the form of aluminosilicate bioglass (B-I) and calciumsilicate bioglasses (Z-5 and Z-8) for Salmonella typhimurium TA 98 and TA 100 in the microplate reverse mutation test. The bioglasses were extracted with 10 cm^3 of dimethyl sulfoxide (DMSO), shaken at 250 rpm for 2 g of B-I and Z-8 bioglass and 1 g of Z-5 bioglass for 72 h at 37°C. Extracts of bioglasses were introduced to the test in the form of solutions in DMSO. They were partially diluted, so that during the exposure 0.25-8.0 mg/cm^3 dose of B-I and Z-8 bioglasses and 0.125-8.0 mg/cm^3 dose of Z-5 bioglass were obtained. Tests were carried out with and without metabolic activation at 30% of S9 fraction.

B-I bioglass caused a reversion of mutations in the TA 100 strain in the presence of S9 fraction. This suggests that indirect mutagens occurred in B-I bioglass that cause base substitution mutations, which TA100 strain detect. Literature data suggests that this could be a consequence of the combined effect of the components of this bioglass and the remains of the substrates used to produce them. Z-5 and Z-8 bioglasses did not result in the reversion of the mutation against any of the test strains used.

The results indicate that there should be further study of Z-5 and Z-8 bioglasses prior to their clinical application, and that B-I bioglass should not be used in the surgical treatment of periodontal disease.

Keywords: *calciumsilicate bioglass, aluminosilicate bioglass, biomaterial, reverse mutation test, mutagenicity*

[Engineering of Biomaterials 135 (2016) 21-27]

Wprowadzenie

W stomatologii problemem są choroby przyzębia. Prowadzą one do tworzenia kieszonek, recesji dziąsła i utraty kości. Agresywną ich postać leczy się stosując antybiotykoterapię ogólną lub miejscową. W najbardziej zaawansowanej fazie choroby oprócz zlikwidowania przyczyny bakteryjnej zachodzi konieczność regeneracji tkanek kostnych przy zastosowaniu metod chirurgicznych. Obecnie do wypełniania ubytków kostnych w chirurgii szczękowo-twarzowej stosuje się m.in. granule bioaktywnego szkła Biogran. Wpływa ono na zwiększoną proliferację osteoblastów (komórek kościotwórczych), ale nie działa antybakteryjnie [1]. Pierwsze najlepiej poznane bioaktywne szkło 45S5 o składzie chemicznym (% wagowy): 24,5% Na_2O, 24,5% CaO, 45% SiO_2, 6% P_2O_5 [2] zostało opracowane przez Hencha i od 1985 roku jest stosowane klinicznie jako Bioglass®. W kolejnej generacji bioszkieł zastosowano metodę zol-żel, która pozwala wytwarzać bioaktywne szkła nawet przy zwiększonym udziale SiO_2, co nie zawsze jest możliwe w metodzie wysokotemperaturowej [3]. Ponadto bioszkła wytwarzane tą metodą mogą mieć postać porowatej matrycy umożliwiającej dostarczanie w sposób kontrolowany np. czynnika bakteriobójczego. Może to być szczególnie przydatne w trakcie chirurgicznego leczenia przyzębia [4]. Ze względu na zagrożenie bakteryjne podczas regeneracji tkanek kostnych w jamie ustnej nadal podejmowane są prace mające na celu tworzenie nowych lub modyfikację istniejących biomateriałów oraz nadawania im właściwości bakteriobójczych [5,6]. Jako czynnik bakteriobójczy najczęściej wykorzystuje się srebro gdyż jego działanie znane jest od stuleci, a mechanizmy oddziaływania na mikroorganizmy zostały wyjaśnione i udokumentowane. Oprócz srebra zdolnościami bakteriobójczymi cechują się również jony innych metali np. miedzi, cyku, złota, ceru [7-9].

Niektóre z materiałów, które potencjalnie mogłyby być zastosowane jako materiały medyczne zawierają substancje wykazujące różne rodzaje toksyczności. Jednym z nich jest genotoksyczność, polegająca na powodowaniu mutacji – trwałych, dziedziczących się zmian substancji dziedzicznej (DNA). Niektóre mutacje mogą indukować powstawanie nowotworów, czyli kancerogenezę. Dlatego przed wprowadzeniem nowych materiałów medycznych do powszechnego zastosowania poddaje się je badaniom pozwalającym na określenie ich właściwości genotoksycznych. Jednym z wielu biotestów pozwalających na określenie aktywności mutagennej badanych próbek jest test Amesa [10,11]. Ze względu na znaczną wiarygodność uzyskiwanych wyników, krótki czas oczekiwania na wynik, relatywnie niską pracochłonność i materiałochłonność należy on do najpowszechniej stosowanych testów na genotoksyczność. Jest on rekomendowany m.in. do badania genotoksyczności wyrobów medycznych [12,13].

Dlatego celem prezentowanej pracy było określenie mutagenności bioszkieł: wapniowokrzemianowego B-I oraz glinokrzemianowych Z-5 i Z-8 wobec *Salmonella typhimurium* w teście Amesa. O wyborze tych bioszkieł do badania genotoksyczności zadecydowały ich nietoksyczność [14] oraz najwyższa skuteczność przeciwbakteryjna spośród badanych bioszkieł [15].

Introduction

Periodontal disease is a problem in dentistry, and leads to the creation of pockets, gingival recession and bone loss. The aggressive characteristics of periodontal disease are treated using general or local antibiotic therapy; in the most advanced stages of the disease it is necessary to regenerate bone tissue using surgical methods in addition to eliminating the bacterial causes. Currently, bioactive granules of Biogran glass, among others, are used in maxillofacial surgery for filling bone defects. These effect an increased proliferation of osteoblasts (osteogenic cells), but do not have an antibacterial effect [1]. The best known 45S5 bioactive glass has a chemical composition (% by weight) of 24.5% Na_2O, 24.5% CaO, 45% SiO_2, 6% P_2O_5 [2]. This was developed by Hench and has been used clinically as Bioglass® since 1985. The sol-gel method was applied to the next generation of bioglass, for producing bioactive glass, as even with the increased involvement of SiO_2 that is not always possible in the high-temperature method [3]. Furthermore, bioglass manufactured by this method may take a porous matrix form, which allows the supply, for example, of a bactericidal agent in a controlled way. This can be especially useful during periodontal surgical treatment [4]. Due to the risk of bacterial contamination during the regeneration of bone tissue in the oral cavity, studies are continually being undertaken with a view to creating new or modifying existing biomaterials and providing them with bactericidal properties [5,6]. Silver has been most commonly used as a bactericidal agent, as its effect has been known for centuries, and its mechanisms of influence on microorganisms have been well documented. In addition to silver, other metal ions such as copper, zinc, gold and cerium are characterized by their bactericidal capacity [7-9].

Some of the materials that could potentially have medical uses contain substances exhibiting various types of toxicity. One of them is genotoxicity. It consists in causing the mutations – permanent, inheritable changes in hereditary substance (deoxyribonucleic acid - DNA). Some mutations can induce cancer, namely carcinogenesis. Therefore, before the introduction of new medical materials for widespread applications, they are examined to determine the genotoxic properties. The Ames test is one of the many bioassays for identifying the mutagenic activity of tested specimens [10,11]. It is the most widely used genotoxity test due to the considerable credibility of the results, a short waiting period, and a relatively low workload and material consumption. It is recommended, among others, in genotoxicity studies of medical products [12,13].

Therefore, the aim of this study was to determine the mutagenicity of B-I calciumsilicate and Z-5 and Z-8 aluminosilicate bioglasses for *Salmonella typhimurium* in the Ames test. Their non-toxicity determined the choice of bioglasses for genotoxicity studies [14] and the highest antibacterial effectiveness among the analyzed bioglasses [15].

Materiały i metody

Badane bioszkła

Badaniu poddano bioszkła (TABELA 1), które wytworzono metodą zol-żel wykorzystując substraty: ortokrzemian tetraetylu (TEOS) jako prekursor krzemionki oraz izopropylan glinu, czterowodny azotan(V) wapnia, fosforan(V) trietylu i azotan(V) srebra. We wcześniejszych doniesieniach literaturowych podano warunki syntezy oraz właściwości fizykochemiczne tych bioszkieł obejmujące m.in. morfologię ziaren i półilościową mikroanalizę powierzchni [16] oraz cytotoksyczność i skuteczność przeciwbakteryjną [14,15].

Odczynniki do testów biologicznych zakupiono w firmie Sigma-Aldrich**:** uwodniona dwusodowa sól D-glukozo-6-fosforanu(V) CAS 3671-99-6; chlorek(I) magnezu sześciowodny CAS 7791-18-6; sól sodowa fosforanu(V) dinukleotytu β-nikotyamidoadeninowego CAS 698999-85-8; chlorek(I) potasu CAS 7447-40-7; fosforan (V) sodu jednozasadowy CAS 7558-80-7, wodorofosforan(V) disodu CAS 7558-79-4, dimetylosulfotlenek(IV) (DMSO) CAS 67-68-5. Pozostałe materiały do testu mikropłytkowego Amesa zostały dostarczone przez firmę Xenometrix by Endotell. W skład zestawu wchodziły: szczepy *Salmonella typhimurium* TA 98 i TA 100, płynne podłoża mikrobiologiczne: wzrostowe, ekspozycyjne i indykacyjne, ampicylina, frakcja mikrosomalna wątroby szczurów aktywowana Aroclor 1254 oraz kontrolne mutageny pozytywne: 2-nitrofluorenon (2-NF), N-tlenek 4-nitrochinoliny (4-NQ), 2-aminoantracen (2-AA) oraz mikropłytki 24, 96 i 384-dołkowe.

TABELA 1. Skład tlenkowy badanych bioszkieł.
TABLE 1. The oxide compositions of tested bioglasses.

Bioszkło Bioglass	Zawartość, wag. % Content, wt%				
	SiO_2	Al_2O_3	CaO	P_2O_5	Ag_2O
Z-5	95.7	0.8	-	-	3.5
Z-8	89.0	7.5	-	-	3.5
B-I	60.0	-	37.0	2.0	1.0

Ekstrakcja

Zgodnie z zaleceniami PN-EN ISO 10993-12 *Biologiczna ocena wyrobów medycznych. Część 12. Przygotowanie próbki i materiały odniesienia* bioszkła B-I i Z-8 ekstrahowano w DMSO stosując proporcję 2 g na 10 cm^3 rozpuszczalnika, wytrząsając z prędkością oscylacji 250 rpm przez 72 h w temperaturze 37°C. W przypadku bioszkła Z-5, które pochłaniało więcej rozpuszczalnika konieczna była zmiana proporcji przez podwojenie ilości DMSO. W celu umożliwienia precyzyjnego dozowania badanych próbek do badań biologicznych ekstrakt oddzielono od zawiesiny przez wirowanie. Wyciąg sterylizowano przez filtrację.

Wykonanie testu

Genotoksyczność bioszkieł badano mikropłytkowym testem Amesa firmy Xenometrix by Endotell z zastosowaniem szczepów *Salmonella typhimurium* TA 98 i TA 100 (Ames MPF™ 98/100). Wykonano testy bez i z aktywacją metaboliczną 30% frakcją mikrosomalną wątroby szczurów S9. Stosowano procedurę opisaną w instrukcji producenta testu. Została ona oparta na pracach [10] oraz [11], z uwzględnieniem różnic procedury spowodowanych wykonaniem testu w podłożach płynnych na mikropłytkach, a nie na podłożu Vogel-Bonnera na szalkach Petriego.

Ekstrakty bioszkieł wprowadzano do testu w postaci roztworów w DMSO. Rozcieńczano je połowicznie, tak aby w czasie ekspozycji uzyskać dawki bioszkieł B-I i Z-8 (0,25, 0,5, 1, 2, 4, 8) mg/cm^3 mieszaniny podczas ekspozycji, a bioszkła Z-5 (0,125, 0,25, 0,5, 1, 2, 4, 8) mg/cm^3. Bakterie testowe były eksponowane na działanie 6 rozcieńczeń badanej próbki przez 90 minut w mikropłytkach 24-dołkowych w 3 powtórzeniach dla każdego rozcieńczenia.

Materials and Methods

Tested bioglasses

The study involved bioglasses (TABLE 1) obtained by the sol-gel method using the following substrates: tetraethyl orthosilicate (TEOS) as a silica precursor and aluminum isopropoxide, calcium nitrate tetrahydrate, triethyl phosphate and silver nitrate. Synthesis conditions and physicochemical properties of these bioglasses were previously reported in the literature, for example grain morphology and semi-quantitative microanalysis of the surfaces [16] and the cytotoxicity and antibacterial potency [14,15].

Reagents for biological tests were purchased from Sigma-Aldrich (St. Luis, USA): D-glucose 6-phosphate (V) disodium salt hydrate CAS 3671-99-6; magnesium chloride(I) hexahydrate CAS 7791-18-6; β-nicotinamide adenine dinucleotide phosphate(V) sodium CAS 698999-85-8; potassium chloride(I) CAS 7447-40-7; sodium phosphate(V) monobasic CAS 7558-80-7; disodium hydrogen phosphate(V) CAS 7558-79-4; dimethyl sulfoxide(IV) (DMSO) CAS 67-68-5. The remaining materials for the Ames microplate test were provided by Xenometrix by Endotell (Allschwill, Switzerland). The set included TA 98 and TA 100 *Salmonella typhimurium* strains, liquid media (growth, exposure and indicator), ampicillin, the microsomal fraction of rat liver activated Aroclor 1254 and the control of positive mutagens (2-nitro-fluorenone (2-NF), N-oxide, 4-nitroquinoline (4-NQ), 2-amino anthracene (2-AA)) and the 24, 96 and 384 well microplate.

Extraction

In accordance with PN-EN ISO 10993-12 (Biological evaluation of medical devices. Part 12. Sample preparation and reference materials) recommendations, B-I and Z-8 bioglasses were extracted in DMSO using a ratio of 2 g in 10 cm^3 of solvent, shaken at an oscillation rate of 250 rpm for 72 hours at 37°C. In the case of Z-5 bioglass, which absorbed more solvent, it was necessary to change the ratio by doubling the amount of DMSO. The extract was separated from the suspension by centrifugation in order to enable a precise dosing of test samples for biological testing. The extract was sterilized by filtration.

Carrying out the test

The genotoxicity of bioglasses were provided by the Ames Xenometrix by Endotell microplate test using TA 98 and TA 100 *Salmonella typhimurium* strains (Ames MPF™ 98/100). Tests were carried out with and without metabolic activation of 30% rat liver S9 microsomal fraction. The procedure described in the manufacturer's instructions test was applied, based on studies [10] and [11], taking into account the differences caused by undertaking the test procedure in the liquid media in microplates and not on the Vogel-Bonner medium on a Petri dishes.

Extracts of bioglasses were introduced into the test as solutions in DMSO. They were partially diluted to obtain B-I and Z-8 bioglass doses of (0.25, 0.5, 1, 2, 4, 8) mg/cm^3 of the mixture during exposure and Z-5 bioglass dose of (0.125, 0.25, 0.5, 1, 2, 4, 8) mg/cm^3. The test bacteria were exposed to six dilutions of test samples for 90 min in a 24-well microplate in triplicate for each dilution.

Ekspozycję prowadzono w 3 powtórzeniach w temperaturze 37°C wytrząsając z prędkością oscylacji 250 rpm. Przed ekspozycją do każdego dołka płytki 24-dołkowej dodawano kolejno 10 µl roztworu próbki w DMSO i 240 µl zawiesiny bakterii testowych w podłożu do ekspozycji (bez lub z dodatkiem frakcji S9 mix). Po zakończeniu ekspozycji do każdego dołka płytki 24-dołkowej dodawano 2,8 cm^3 podłoża wskaźnikowego, a następnie przesiewano po 50 µl do mieszaniny hodowlanej z każdego dołka płytki 24-dołkowej do 48 dołków płytki 384-dołkowej. Płytki 384-dołkowe inkubowano przez 48 godzin w temperaturze 37°C w warunkach tlenowych, wytrząsając z prędkością oscylacji 250 rpm. Po upływie 48 godzin odczytywano wyniki testu licząc osobno dla każdego rozcieńczenia badanej próbki dołki z rewertantami. Ich obecność określano na podstawie zmiany koloru podłoża indykacyjnego z fioletowego na żółte albo obecności na dnie dołka widocznej kolonii bakterii.

Wynik testu, zgodnie z procedurą opisaną w instrukcji producenta testu, uznawano za dodatni, gdy liczba dołków zawierających rewertanty była co najmniej trzykrotnie większa niż w kontroli negatywnej. Do analizy statystycznej wyników wykorzystywano arkusz kalkulacyjny Excel dostarczony przez producenta testu. Statystyczną istotność różnic liczby rewertantów między badanymi próbkami a kontrolami negatywnymi badano jednostronnym testem t-Studenta. Różnice uznawano za statystycznie istotne przy p≤0,05. Zgodnie z procedurą, wyniki testu uznawano za wiarygodne, gdy średnia liczba dołków pozytywnych (z rewertantami) w kontroli negatywnej nie przekraczała 8 dla szczepu *Salmonella typhimurium* TA 98 i 12 dla szczepu *Salmonella typhimurium* TA 100 a w kontroli pozytywnej wynosiła co najmniej 25.

Wyniki i dyskusja

Bioszkło wapniowokrzemianowe B-I wykazywało aktywność mutagenną wobec szczepu TA100 z aktywacją metaboliczną frakcją S9, nie wykazywało aktywności mutagennej wobec szczepu TA100 bez aktywacji metabolicznej ani wobec szczepu TA98 bez i z aktywacją metaboliczną. Pozwala to wnioskować, że bioszkło B-I zawierało mutageny pośrednie powodujące powstawanie mutacji podstawiania par zasad na wykrywanie których pozwala szczep TA100. Nie zawierało ono mutagenów bezpośrednich powodujących powstawanie mutacji podstawiania par zasad ani mutagenów bezpośrednich i pośrednich powodujących powstawanie mutacji zmiany fazy odczytu, na wykrywanie których pozwala szczep TA98 (TABELA 2).

Exposure was carried out at 37°C, shaken at an oscillation speed of 250 rpm. 10 µl of the sample solution in DMSO, 240 µl of bacterial suspension in the exposure medium (with or without S9) were added before exposure to each one of the 24 wells. 2.8 cm^3 of indicator medium was added after exposure to each well and then 50 ml of the mixture from each well was sieved to one of 48 wells of a 384-well plate. The 384-well plates were incubated for 48 h at 37°C in aerobic conditions, shaken at an oscillation speed of 250 rpm. After 48 h, the test results were read separately and counted for each dilution of the sample holes from the revertants. Their presence was determined by the indicative substrate color change from purple to yellow, or the presence of bacteria colonies visible at the bottom of the hole.

Tests were performed according to the procedure described in the manufacturer's instructions; the result was positive when the number of holes containing revertants was at least three times greater than the negative control. An Excel spreadsheet provided by the manufacturer of the test was used for statistical analysis. The statistical significance of the differences in the number of revertants between test samples and negative controls were studied in a unilateral t-test and were considered significant at $p \leq 0.05$. According to the procedure, the test results were considered reliable because the average number of positive holes (from the revertant) did not exceed 8 in the negative control for a TA 98 and 12 for the *Salmonella typhimurium* strain, and did not exceed 25 for the TA 100 *Salmonella typhimurium* strain in the positive control.

Results and Discussions

B-I calciumsilicate bioglass showed mutagenic activity against the TA100 strain with metabolic activation of the S9 fraction, and did not demonstrate mutagenic activity against the TA100 strain without metabolic activation or the TA98 strain with and without metabolic activation. This indicates that B-I bioglass included indirect mutagens that cause base-substitution mutations, which TA100 strain detect. They did not include direct mutagens causing base-substitution mutations and direct and indirect mutagens caused frame-shift mutations, the detection of which allows the TA98 strain (TABLE 2).

TABELA 2. Wyniki badania genotoksyczności bioszkła B-I.
TABLE 2. The results of genotoxicity tests of B-I bioglass.

Stężenie Concentration [mg/cm^3]	Liczba dołków pozytywnych (średnia i odchylenie standardowe) The number of positive holes (mean and standard deviation)			
	TA 98		TA 100	
	-S9	+S9	-S9	+S9
0	1.33 ± 1.00	1.67 ± 0.58	4.22 ± 1.72	6.11 ± 1.96
0.25	0.67 ± 0.58	1.67 ± 0.58	5.00 ± 3.46	26.67 ± 6.51*
0.5	0.67 ± 0.58	2.33 ± 2.08	2.67 ± 0.58	28.00 ± 2.65*
1	0.67 ± 0.58	2.67 ± 2.52	3.67 ± 0.58	29.33 ± 4.16*
2	1.67 ± 0.58	1.67 ± 1.15	4.67 ± 2.52	29.67 ± 8.08*
4	0.33 ± 0.58	2.33 ± 1.15	4.00 ± 1.00	28.00 ± 3.00*
8	1.00 ± 1.00	1.00 ± 1.00	3.00 ± 1.00	23.67 ± 5.51*
kontrola pozytywna positive control	32.33 ± 3.06	47.67 ± 0.58	46.67 ± 0.58	48.00 ± 0.00
*p<0.0001				

Genotoksyczność niektórych składników bioszkieł opisanych w tej pracy oraz ich prekursorów była wcześniej badana indywidualnie. Spośród tlenków wchodzących w skład chemiczny bioszkła B-I testem rewersji mutacji z wynikiem negatywnym badany był tlenek wapnia [17,18]. W dostępnej literaturze brakuje natomiast informacji o badaniu tym testem pozostałych składników. Chroniczna inhalacja tlenkiem krzemu powodowała u szczurów powstanie nowotworu płuc gdy miał on postać krystaliczną, nie powodowała natomiast powstania nowotworu gdy miał on postać amorficzną [19].

W bioszkle B-I mogły też pozostać śladowe ilości substratów użytych do jego wytworzenia. Niektóre z nich powodują powstawanie różnych mutacji. We wcześniejszych badaniach rewersję mutacji punktowych u *Salmonella typhimurium* powodował fosforan(V) trietylu [20]. TEOS i azotan(V) srebra nie powodowały rewersji mutacji u *Salmonella*. Azotan(V) srebra powodował powstawanie mutacji w teście SMART i fragmentację DNA u *Drosophila melanogaster*, nie powodował natomiast powstawania aberracji chromosomowych w limfocytach ludzkich [21-24]. Zebrane dane literaturowe wskazują, że rewersja mutacji w szczepie TA 100 w obecności frakcji S9 powodowana przez bioszkło B-I mogła być następstwem łącznego działania jego składników oraz pozostałości substratów użytych do ich wytworzenia.

Bioszkła glinokrzemianowe Z-5 i Z-8 nie wykazywały aktywności mutagennej wobec obu zastosowanych szczepów testowych *Salmonella typhimurium* bez i z aktywacją metaboliczną frakcją S9 w badanym zakresie stężeń (TABELE 3 i 4). Pozwala to wnioskować, że badane bioszkła nie zawierały mutagenów bezpośrednich ani pośrednich powodujących powstawanie mutacji zmiany fazy odczytu i podstawiania par zasad na wykrywanie których pozwalają szczepy *Salmonella typhimurium* TA 98 i TA 100.

The genotoxicity of some individual bioglass components described here and their precursors has been previously studied. Calcium oxide was among the oxides constituting the chemical B-I bioglass mutation reversion test with negative results in the test [17,18]. There is a need for information about testing of the remaining ingredients in this assay. Chronic inhalation of crystalline silica induced rat lung cancer formation when it took a crystalline form, but did not induce cancer formation when it took an amorphous form [19].

B-I bioglass could also contain trace amounts of substrates used to make it. Some of them give rise to different mutations. In previous studies, the reversing point mutations in *Salmonella typhimurium* were caused by triethyl phosphate [20]. TEOS and silver nitrate did not cause the reversion of mutations in *Salmonella*. Silver nitrate generated mutations in the SMART test and DNA fragmentation in *Drosophila melanogaster*, but did not cause formation of chromosomal aberrations in human lymphocytes [21-24]. The collected literature data indicate that reversion of mutations in the TA 100 strain in the presence of S9 caused by B-I bioglass could be a consequence of the combined effect of its components and the substrates remains used to obtain it.

Z-5 and Z-8 aluminosilicate bioglasses did not exhibit mutagenic activity applied to the *Salmonella typhimurium* strains tests with and without metabolic activation of S9 fraction in the tested concentrations (TABLES 3 and 4). This suggests that the tested bioglasses did not contain direct or indirect mutagens causing a frame-shift mutation and base-substitution mutation for the detection that allows TA 98 and TA 100 strains of *Salmonella typhimurium*.

TABELA 3. Wyniki badania genotoksyczności bioszkła Z-5.
TABLE 3. The results of genotoxicity tests of Z-5 bioglass.

Stężenie Concentration [mg/ cm^3]	Liczba dołków pozytywnych (średnia i odchylenie standardowe) The number of positive holes (mean and standard deviation)			
	TA 98		TA 100	
	-S9	+S9	-S9	+S9
0	1.33 ± 1.00	1.73 ± 0.65	4.22 ± 1.72	6.11 ± 1.96
0.125	1.00 ± 1.00	3.00 ± 1.73	4.67 ± 1.15	6.67 ± 3.51
0.25	0.67 ± 1.15	2.00 ± 1.00	3.00 ± 1.73	5.67 ± 1.53
0.5	1.33 ± 1.53	2.33 ± 1.15	3.67 ± 0.58	7.00 ± 1.00
1	0.67 ± 1.15	2.00 ± 1.00	3.00 ± 1.00	9.00 ± 2.65
2	0.33 ± 0.58	2.00 ± 0.00	3.00 ± 1.73	8.33 ± 2.08
4	0.67 ± 0.58	1.67 ± 0.58	3.33 ± 1.15	6.00 ± 3.46
8	1.33 ± 1.15	2.00 ± 1.00	3.67 ± 0.58	6.33 ± 1.53
kontrola pozytywna positive control	34.33 ± 4.16	48.00 ± 0.00	47.67 ± 0.58	47.67 ± 0.58

TABELA 4. Wyniki badania genotoksyczności bioszkła Z-8.
TABLE 4. The results of genotoxicity tests of Z-8 bioglass.

Stężenie Concentration [mg/ cm^3]	Liczba dołków pozytywnych (średnia i odchylenie standardowe) The number of positive holes (mean and standard deviation)			
	TA 98		TA 100	
	-S9	+S9	-S9	+S9
0	1.33 ± 1.00	1.73 ± 0.65	4.22 ± 1.72	6.11 ± 1.96
0.25	1.00 ± 0.00	4.00 ± 1.73	3.00 ± 1.00	7.00 ± 1.00
0.5	0.33 ± 0.58	2.00 ± 1.00	7.00 ± 2.00	7.67 ± 2.08
1	1.33 ± 0.58	2.33 ± 1.15	5.00 ± 2.65	4.00 ± 1.00
2	0.33 ± 0.58	2.00 ± 1.00	5.33 ± 0.58	4.33 ± 3.51
4	0.33 ± 0.58	2.00 ± 0.00	4.00 ± 3.46	6.33 ± 1.53
8	0.67± 0.58	1.67 ± 0.58	3.67 ± 2.08	8.33 ± 2.08
kontrola pozytywna positive control	33.00 ± 2.00	48.00 ± 0.00	47.33 ± 0.58	47.67 ± 0.58

Tlenek glinu wchodzący w skład bioszkieł Z-5 i Z-8 nie wykazywał genotoksyczności w teście Amesa [17], także jako nanomateriał [25,26]. Nie powodował on obniżenia indeksu mitotycznego, powodował natomiast powstawanie mikrojąder i aberracji chromosomowych w erytrocytach polichromatycznych szpiku kostnego szczurów [25]. Pozostałe składniki tego bioszkła i substraty użyte do jego wytworzenia były takie same, jak w wapniowokrzemianowym bioszkle B-I. Wśród jego składników nie było tylko tlenku wapnia, zatem czterowodny azotan(V) wapnia nie był używany do jego wytworzenia.

Z badanych bioszkieł uwalniane są jony srebra, które wykazują działanie antybakteryjne. Srebro mogło zostać wbudowane w strukturę bioszkła a także występować jako nanocząstki metalu na powierzchni ziaren, co potwierdzają badania TEM [27]. Antybakteryjne działanie jonów srebra polega m.in. na wchodzeniu w reakcje z zasadami azotowymi. Prowadzi to do powstania skondensowanej formy kwasu nukleinowego. W takiej formie nie może dojść do powielenia materiału genetycznego [28,29]. Srebro blokuje też enzymy oksydacyjne łańcucha oddechowego. W odpowiedzi dochodzi do wzmożonej produkcji wolnych rodników, które powodują uszkodzenia komórki [30,28]. Mogą one też powodować powstawanie mutacji [31]. W teście Amesa nanosrebro nie wykazywało genotoksyczności, powodowało jednak powstawanie mikrojąder w limfoblastoidach ludzkich TK6 [32]. Może ono zatem być genotoksyczne dla organizmów eukariotycznych, w tym dla człowieka, mimo negatywnego wyniku w teście bakteryjnym.

Wnioski

Uzyskane wyniki wskazywały na występowanie w bioszkle wapniowokrzemianowym B-I mutagenów pośrednich powodujących mutacje podstawiania par zasad. Preparat ten nie powinien zatem być stosowany w chirurgicznym leczeniu chorób przyzębia. Bioszkła glinokrzemianowe Z-5 i Z-8 nie wykazywały aktywności mutagennej wobec *Salmonella typhimurium* TA 98 i TA 100 w teście Amesa bez i z aktywacją metaboliczną. Oznacza to, że nie powodują one powstawania mutacji zmiany fazy odczytu i podstawiania par zasad, na wykrywanie których pozwalają zastosowane szczepy. Pozwala to rekomendować bioszkła Z-5 i Z-8 do dalszych badań poprzedzających ich kliniczne zastosowanie.

Podziękowania

Praca naukowa finansowana ze środków na naukę Ministerstwa Nauki i Szkolnictwa Wyższego jako projekt badawczy rozwojowy Nr R08 010 02.

Aluminum oxide forming the Z-5 and Z-8 bioglasses composition was not genotoxic in the Ames test [17], or as a nanomaterial [25,26]. It did not cause a reduction in mitotic index, but induced the formation of micronuclei and chromosomal aberrations in the polychromatic erythrocytes of bone marrow of rats [25]. The remaining components of these bioglasses and substrate used in their manufacture are the same as B-I calciumsilicate bioglass. Only calcium oxide was not among its components, which means that calcium nitrate tetrahydrate had not been used for its manufacture.

Silver ions that exhibit antibacterial activity are released from the tested bioglasses. Silver could be built into the structure of bioglass and occurred as nanoparticles of metal on grains surfaces confirmed by TEM [27]. The antibacterial activity of silver ions relies, among others, on nitrogen bases entering in the reactions. This leads to the formation of condensed forms of nucleic acid. As such, there can be no duplication of genetic material [28,29]. Silver also blocks oxidative enzymes of electron transport chain. In response, there is an increased production of free radicals that damage cells [30,28]. They can also cause mutations [31]. Nanosilver showed no genotoxicity in the Ames test; however it resulted in the formation of micronuclei in the humanTK6 lymphoblastic blastoid [32]. It may be genotoxic to eukaryotic organisms including humans, despite negative result obtained in the bacterial test.

Conclusions

The results indicated that the presence of intermediate mutagens in the B-I calciumsilicate bioglass cause base-substitution mutations. This formulation should therefore not be used in the surgical treatment of periodontal diseases. The Z-5 and Z-8 aluminosilicate bioglasses did not exhibit mutagenic activity against TA 98 and TA 100 *Salmonella typhimurium* in the Ames test, with and without metabolic activation. This means that they do not cause frame-shift and base substitution mutations, which the applied strain allows for detection. Thus, there should be further study of Z-5 and Z-8 bioglasses prior to their clinical application.

Acknowledgments

The study was financed by Polish Ministry of Science and Higher Education (project no. R08 010 02).

Pismiennictwo

[1] http://www.atekgroup.com/upfiles/image/dayou/Biogran%20(ART668B).pdf
[2] Crovace M.C., Souza M.T., Chinaglia C.R., Peitl O., Zanotto E.D.: Biosilicate – A multipurpose, highly bioactive glass-ceramic. In vitro, in vivo and clinical trials. Journal of Non-Crystalline Solids 432 (2016) 90-110.
[3] Saravanapavan P., Hench L.: Low-temperature synthesis, structure, and bioactivity of gel-derived glasses in the binary CaO-SiO_2 system. Journal of Biomedical Materials Research 54 (2001) 608-618.
[4] Balamurugan A., Balossier G., Laurent-Maguin D., Pina S., Rebelo A.H.S., Faure J., Ferreira J.M.F.: An in vitro biological and anti-bacterial study on a sol-gel derived silver-incorporated bioglass system. Dental Materials 24 (2008) 1343-1351.
[5] Ciołek L. Karaś J,. Olszyna A., Traczyk S.: New silver-containing bioglasses. Engineering of Biomaterials 77-80, (2008) 25-27.
[6] Zhu H., Hu Ch., Zhang F., Feng X., Li J., Liu T., Chen J., Zhang J.: Preparation and antibacterial property of silver-containing mesoporous 58S bioactive glass. Materials Science and Engineering C 42 (2014) 22-30.
[7] Kim T.N., Feng Q.L., Kim J.O., Wu J., Wang H., Chen G.C., Cui F.Z.: Antimicrobial effects of metal ions (Ag^+, Cu^{2+}, Zn^{2+}) in hydroxyapatite. Journal of Materials Science: Materials in Medicine 9 (1998) 129-134.
[8] Cui Y., Zhao Y., Tian Y., Zhang W., Lu X., Jiang X.: The molecular mechanism of action of bactericidal gold nanoparticles on *Eschericha coli*. Biomaterials 33 (2012) 2327-2333.
[9] Goh Y.F., Alshemary A.Z., Akram M., Kadir M.R.A., Hussain R.: In-vitro characterization of antibacterial bioactive glass containing ceria. Ceramics International 40 (2014) 729-737.
[10] Maron D.M., Ames B.N.: Revised methods for the *Salmonella* mutagenicity test. Mutation Research 113 (1983) 173-215.
[11] Mortelmans K., Zeiger E.: The *Salmonella*/microsome mutagenicity assay. Mutation Research 455 (2000) 29-60.
[12] Polska Norma PN-EN ISO 10993-12. Biologiczna ocena wyrobów medycznych. Część 12. Przygotowanie próbki i materiały odniesienia.
[13] Polska Norma PN-EN ISO 10993-3. Biologiczna ocena wyrobów medycznych. Część 3. Badania genotoksyczności, rakotwórczości i toksyczności reprodukcyjnej.
[14] Ciołek L., Karaś J., Olszyna A. Zaczyńska E., Czarny A., Żywicka B.: *In vitro* studies of cytotoxicity of bioglass containing silver. Engineering of Biomaterials 89-91 (2009) 91-93.
[15] Ciołek L., Karaś J., Olszyna A., Zaczyńska E., Czarny A., Żywicka B.: *In vitro* antibacterial activity of silver silver-containing bioglasses. Engineering of Biomaterials 100-101 (2010) 21-23.
[16] Ciołek L., Karaś J., Olszyna A.: Badania właściwości fizykochemicznych bioszkieł domieszkowanych srebrem wytworzonych metodą zol-żel. *Prace Instytutu Szkła, Ceramiki, Materiałów Ogniotrwałych i Budowlanych* 3 (2009) 15-25.
[17] Rim K.-T., Kim S.-J., Kim J.-G., Kim H.-Y., Yang J.-S.: Bacterial Reverse Mutation (AMES) Test of Aluminium Oxide, Calcium Oxide, and Sodium Tetraborate. Journal of the Korean Society for Environmental Analysis 12(3) (2009) 196-203.

References

[18] Sawai J., Kojima H., Kano F., Igarashi H., Hashimoto A., Kawada E., Kokugan T., Shimizu M.: Ames assay with Salmonella typhimurium TA 102 for mutagenicity and antimutagenicity of metallic oxide powders having antibacterial activities. World Journal of Microbiology and Biotechnology 14 (1998) 773-775.
[19] Johnston C.J., Driscoll K.E., Finkelstein J.N., Baggs R., O'Reilly M.A., Carter J., Gelein R., Obersdörter G.: Pulmonary Chemokine and Mutagenic Responses in Rats after Subchronic Inhalation of Amorphous and Cristalline Silica. Toxicological Sciences 56 (2000) 405-413.
[20] Dyer K.F., Hanna P.J.: Comparative mutagenic activity and toxicity of trietylphosphate and dichlorvos in bacteria and Drosophila. Mutation Research 21 (1973) 175-177.
[21] Reutova N.V., Shevtschenko V.A.: Silver as a potential mutagen. Genetica 27(7) (1991) 1280-1284.
[22] Sumitha R., Swarna R., Priyanka V., Deepa P. V.: *In vivo* and *in vitro* genotoxicity analysis of silver nitrate. Drosophila Information Service 96 (2013) 40-46.
[23] Lionti K., Séverin I., Dahbi L., Toury B., Chagnon M.Ch.: *In vitro* genotoxicity assessment of MTES, GPTES and TEOS, three precursors intended for use in food contact coatings. Food and Chemical Toxicology 65 (2014) 76-81.
[24] Butler K.S., Peeler D. J., Casey B.J., Dair B.J., Elespuru R.K.: Silver nanoparticles: correlating nanoparticle size and cellular uptake with genotoxicity. Mutagenesis 30 (2015) 577-591.
[25] Balasubramanyam A., Sailaja N., Mahboob M., Rahman M.F., Hussain S.M., Grover P.: *In vitro* mutagenicity assessment of aluminium oxide nanomaterials using the *Salmonella*/microsome assay. Toxicology in Vitro 24 (2010) 1871-1876.
[26] Pan X., Redding J., Wiley P.A., Wen L., McConnell J.S., Zhang B.: Mutagenicity evaluation of metal oxide nanoparticles by the bacterial reverse mutation assay. Chemosphere 79 (2010) 113-116.
[27] Ciołek L., Karaś J., Olszyna A., Zaczyńska E., Czarny A., Żywicka B.: Badania właściwości fizykochemicznych i biologicznych in vitro bioszkieł ze srebrem wytworzonych metodą zol-żel. Szkło i Ceramika 61(1) (2010) 2-6.
[28] Yamanaka M., Hara K., Kudo J.: Bactericidal actions of silver ion solution on *Escherichia coli*, studied by energy-filtering transmission electron microscopy and proteomic analysis. Applied and Environmental Microbiology 71 (2005) 7589-7593.
[29] Woo K.J., Koo H.C., Kim K.W., Shin S., Kim S.H., Park Y.H.: Antibacterial activity and mechanism of action of the silver ion in *Staphyloccocus aureus* and *Escherichia coli*. Applied and Environmental Microbiology 74 (2008) 2171-2178.
[30] Matsumura Y., Yoshikata K., Kunisaki S.I., Tsuchido T.: Mode of bactericidal action of silver zeolite and its comparison with that of silver nitrate. Applied and Environmental Microbiology 69 (2003) 4278-4281.
[31] Kim S., Ryu D.Y.: Silver nanoparticle-induced oxidative stress, genotoxicity and apoptosis in cultured cells of animal tissues. Journal of Applied Toxicology 33 (2013) 78-89.
[32] Li Y., Chjen D.H., Yan J., Chen Y., Mittelstaedt R.A., Zhang Y., Biris A.S., Heflich R.H., Chen T.: Genotoxicity of silver nanoparticles evaluated using the Ames test and *in vitro* micronucleus assay. Mutation Research 745 (2012) 4-10.

AGH

STUDIA PODYPLOMOWE
Biomateriały – Materiały dla Medycyny
2016/2017

Organizator: Akademia Górniczo-Hutnicza im. Stanisława Staszica w Krakowie Wydział Inżynierii Materiałowej i Ceramiki Katedra Biomateriałów **Kierownik:** prof. dr hab. inż. Elżbieta Pamuła **Sekretarz:** dr inż. Małgorzata Krok-Borkowicz	**Adres:** 30-059 Kraków, Al. Mickiewicza 30 Pawilon A3, p. 208, 210 lub 501 tel. 12 617 44 48, 12 617 23 38, fax. 12 617 33 71 email: epamula@agh.edu.pl; krok@agh.edu.pl http://www.agh.edu.pl/ksztalcenie/oferta-ksztalcenia/studia-podyplomowe/biomaterialy-materialy-dla-medycyny/

Charakterystyka:
Tematyka prezentowana w trakcie zajęć obejmuje przegląd wszystkich grup materiałów dla zastosowań medycznych: metalicznych, ceramicznych, polimerowych, węglowych i kompozytowych. Słuchacze zapoznają się z metodami projektowania i wytwarzania biomateriałów a następnie możliwościami analizy ich właściwości mechanicznych, właściwości fizykochemicznych (laboratoria z metod badań: elektronowa mikroskopia skaningowa, mikroskopia sił atomowych, spektroskopia w podczerwieni, badania energii powierzchniowej i zwilżalności) i właściwości biologicznych (badania: *in vitro* i *in vivo*). Omawiane są regulacje prawne i aspekty etyczne związane z badaniami na zwierzętach i badaniami klinicznymi (norma EU ISO 10993). Słuchacze zapoznają się z najnowszymi osiągnięciami w zakresie nowoczesnych nośników leków, medycyny regeneracyjnej i inżynierii tkankowej.

Sylwetka absolwenta:
Studia adresowane są do absolwentów uczelni technicznych (inżynieria materiałowa, technologia chemiczna), przyrodniczych (chemia, biologia, biotechnologia) a także medycznych, stomatologicznych, farmaceutycznych i weterynaryjnych, pragnących zdobyć, poszerzyć i ugruntować wiedzę z zakresu inżynierii biomateriałów i nowoczesnych materiałów dla medycyny. Słuchacze zdobywają i/lub pogłębiają wiedzę z zakresu inżynierii biomateriałów. Po zakończeniu studiów wykazują się znajomością budowy, właściwości i sposobu otrzymywania materiałów przeznaczonych dla medycyny. Potrafią analizować wyniki badań i przekładać je na zachowanie się biomateriału w warunkach żywego organizmu. Ponadto słuchacze wprowadzani są w zagadnienia dotyczące wymagań normowych, etycznych i prawnych niezbędnych do wprowadzenia nowego materiału na rynek. Ukończenie studiów pozwala na nabycie umiejętności przygotowywania wniosków do Komisji Etycznych i doboru metod badawczych w zakresie analizy biozgodności materiałów.

Zasady naboru:
Termin zgłoszeń: od 20.09.2016 do 20.10.2016 (liczba miejsc ograniczona - decyduje kolejność zgłoszeń)
Wymagane dokumenty: dyplom ukończenia szkoły wyższej
Osoby przyjmujące zgłoszenia:
prof. dr hab. inż. Elżbieta Pamuła (pawilon A3, p. 208, tel. 12 617 44 48, e-mail: epamula@agh.edu.pl)
dr inż. Małgorzata Krok-Borkowicz (pawilon A3, p. 210, tel. 12 617 23 38, e-mail: krok@agh.edu.pl)
mgr inż. Krzysztof Pietryga (pawilon A3, p. 501, tel. 12 617 47 44, pietryga@agh.edu.pl)

Czas trwania: 2 semestry (od XI 2016 r. do VI 2017 r.) 8 zjazdów (soboty-niedziele) 1 raz w miesiącu Przewidywana data rozpoczęcia: 19 XI 2016 r.	**Opłaty:** 2 600 zł